uc3m | Universidad Carlos III de Madrid

University Degree in Energy Engineering
2018-2019

Bachelor Thesis

"Study of the Refrigeration and Air Filter Systems of Wind Turbine Nacelles in the Desert"

Alberto López Rolo

Carolina Marugán Cruz

Leganés, June 15, 2019

UNIVERSITY CARLOS III DE MADRID

Study of the Refrigeration and Air Filter Systems of Wind Turbine Nacelles in the Desert

by

Alberto López Rolo

A thesis submitted in partial fulfillment for the
degree of Energy Engineering

in the
Escuela Politecnica Superior, UC3M
Department of Thermal and Fluid Engineering

June 2019

Declaration of Authorship

I, Alberto López Rolo, declare that this thesis titled, 'Study of the Refrigeration and Air Filter Systems of Wind Turbine Nacelles in the Desert' and the work presented in it are my own. I confirm that:

- This work was done wholly or mainly while in candidature for a Bachelor Thesis (Trabajo Fin de Grado) at this University.

- Where any part of this thesis has previously been submitted for a degree or any other qualification at this University or any other institution, this has been clearly stated.

- Where I have consulted the published work of others, this is always clearly attributed.

- Where I have quoted from the work of others, the source is always given. With the exception of such quotations, this thesis is entirely my own work.

- I have acknowledged all main sources of help.

- Where the thesis is based on work done by myself jointly with others, I have made clear exactly what was done by others and what I have contributed myself.

Signed: Alberto López Rolo

Date: 15$^{\text{th}}$ of June, 2019

Acknowledgements

UNIVERSITY CARLOS III DE MADRID

Bachelor Thesis (TFG)

Escuela Politecnica Superior, UC3M
Department of Thermal and Fluid Engineering

Energy Engineering

by Alberto López Rolo

In this thesis, the refrigeration and air filtration systems of a nacelle of Wind Energy Conversion Systems (WECS) in desert climates is studied. A comparison between two dust particle filtration systems is performed, in a technical-economical analysis. The solution proposed to improve the air filtration of the refrigeration system consists of, substituting conventional mesh-fiber filters with an Electrostatic Precipitator (ESP). To do this some background is given in dust particle filtration efficiency measurement, as well as a methodology to do the comparison. In addition to that, an investigation on the theoretical principles of electrostatic precipitation is given, and based on that, an experimental ESP is designed. The study will focus on a horizontal axis WECS, placed in a desert climate, specifically in the Arabian Desert, where the most suitable location to place a WECS is chosen, and the climatic conditions data for that place is researched.

Contents

List of Figures

List of Tables

Abbreviations

WECS   **W**ind **E**nergy **C**onversion **S**ystem

ESP   **E**lectro-**S**tatic **P**recipitator

MENA   **M**iddle **E**ast and **N**orth **A**frica

AGL   **A**bove **G**round **L**evel

AEP   **A**nnual **E**nergy **P**roduction

KAU   **K**ing **A**bdulaziz **U**nivesity

Symbols

e	Euro	currency
$\$$	U.S. Dollar	currency
MW	Megawatt	Power
kWh	Kilowatt hour	Energy

Dedicated to my family and friends, who in one way or the other helped me and gave me guidance whenever I asked for it.

Chapter 1

Introduction

1.1 Background

For the last decades cleaner, cheaper and more sustainable energy has dominated the energy generation debate, and how to achieve these goals regarding the current and future energy pool in a global sense, since the pollution of the planet does not just affect locally, but has also a global impact. Regarding this topic, renewable energy sources such as wind and solar have been the most popular answer to this question. As so, developed countries have developed these technologies and, at different degrees, implemented them in their respective energy pools. Ranging from 44.4% in Denmark to 4.8% in countries like France, the percentage of the average annual electricity demand covered by wind in 2017 [1] (see fig. 1.1.a)

However,developing and undeveloped countries, don't have as much resources as are needed for the research and development of these relatively new generation technologies, and therefore lack the capacity to comply with international environmental agreements of cleaner, less pollutant energy generation. For example, in the MENA Region (Middle East and North Africa) the Wind Power installed capacity represents less than 1% of the world's installed capacity (fig. 1.1.b). So, in this thesis, the state of wind energy in the desert climate is investigated, and the problems that lead up from this environment, mainly dust, sand and extreme hot temperatures are studied, and a possible solution or improvement of the filtration and ventilation systems regarding these problems proposed.
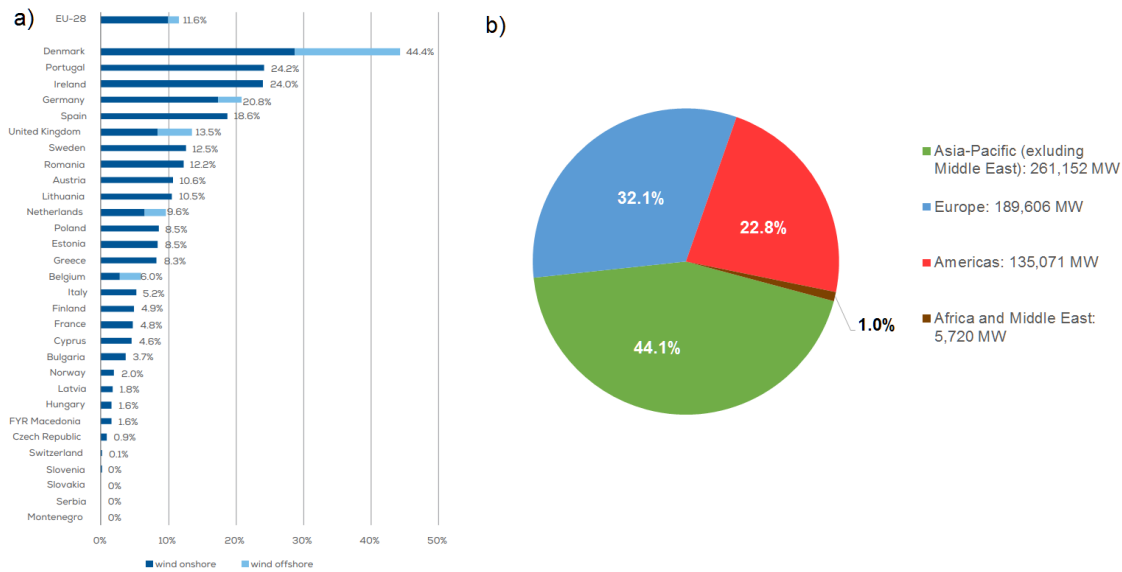
FIGURE 1.1: Percentage of a) the Average Annual Electricity Demand covered by Wind in the EU (2017) [1] and b) Wind Energy Power Installed Capacity, by Regions (2018) [2]

1.2 Motivation

A question that the reader might ask is, why trying to use wind energy in the desert when conditions are so harsh and hostile? Why not use solar instead?, since the hours of sunlight in the desert are 3600 h a year and 75% clear sky. Well, the simple answer is that renewable energy sources are intermittent, and therefore it is recommended to diversify and use different technologies, if possible, to have a more robust and stable energy mix. And another, reason is that wind farms take up a lot of space and have downsides for people living nearby, for example, noise or visual contamination. Being the desert as inhospitable as it is for human life, the energy potential that could be extracted from it is very high, given that little to nothing else is done in the desert. And for a possible investor, since huge acres of desert are unused, it might be a very cheap real-state investment for the wind farm developer.

The necessity for the specificity of studying refrigeration and air filtration systems of WECS nacelles in desert environments, at a glance, it can be obvious given that the climate conditions are harsher in this environment than in any other, given the extreme temperatures and high presence of dust and sand in the air when the wind blows, given the nature of sand and its close to liquid behavior. It is has been pointed out in the literature that for a commercial WECS placed in the desert: "an appropriate cooling system might be designed and sized based on the resulting environmental thermal load" [11].

Being the Middle East and North Africa (MENA) conditions so specific, it is important for manufacturers, normally foreign to these countries with such different and specific conditions, to understand which are these conditions and improve their WECS design based on them, to cover the demand that the energy market is generating in this region of the world.

1.3   Objectives and scope of the work

The objective of this thesis is to study the improvement of the air filtration and refrigeration system of a WECS Nacelle. In order to accomplish this purpose, the following tasks will be performed:

- Explain and understand how the refrigeration system of a commercial 3 MW WECS works.

- Explain the conditions that pose problems to the WECS Nacelles in the desert climate of Saudi Arabia, related with air filtration and refrigeration systems.

- The viability of replacing the traditionally used mesh-fiber filters for the air filtration system with ESPs will be studied.

1.4   Outline of the bachelor's thesis

- **Chapter 1, INTRODUCTION**, Some background and motivation for the project is given, and the objectives to be accomplish in this study defined.

- **Chapter 2, WIND ENERGY CONVERSION SYSTEMS**, The working principle and basic architecture of a WECS is reviewed, and an explanation of how WECS cooling systems work given.

- **Chapter 3, DUST PARTICLE FILTRATION**, An explanation of which are the possible dust filtration systems that could be used in a WECS, and a method for measuring particle size. Also the methodology for the comparison of two different filtration systems is outlined. This methodology will be followed when performing the comparison in the case study chapter

- **Chapter 4, ELECTROSTATIC PRECIPITATORS**, in this section a comprehensive explanation of what ESPs are, and how they work, accessible for a reader not familiarized with this topic.

- **Chapter 5, CASE STUDY**, here, a specific place in Saudi Arabia is selected, and its environmental conditions researched. Then the theory about ESPs is applied to a real case, to design an experimental ESP suited for a WECS of 3 MW in the Arabian desert. In this chapter the ESP will be compared with the mesh-fiber filter filtration system in terms of performance and in an cost-benefit analysis.

- **Chapter 6, SOCIO-ECONOMIC IMPACT**, A description of how the investigation and development of this thesis can affect the area's social and economic state.

- **Chapter 7, CONCLUSIONS**, in this section, some key conclusions from the study are highlighted, and whether the objectives proposed in the first chapter have been fulfilled.

Chapter 2

Wind Energy Conversion Systems

2.1 WECS Overview

In order to understand the problem that a WECS has on the dessert, an overview of the architecture of the WECS nacelle and of its internal components is explained here, so that the key functions and the generation of heat that each part produces is properly understood.
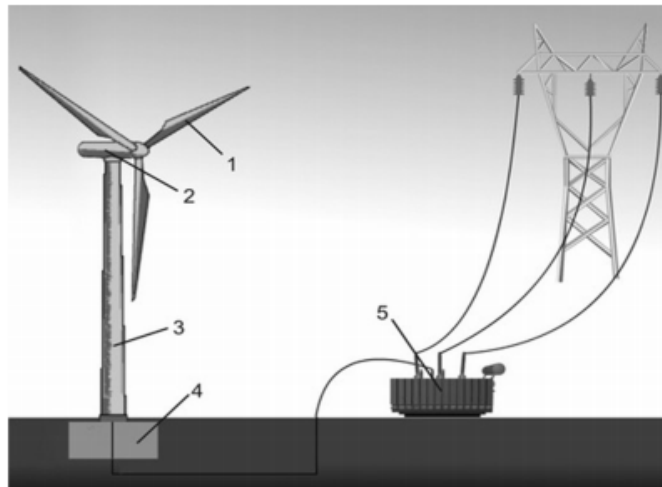
FIGURE 2.1: Sketch of a WECS connected to a power system: 1, impeller; 2, nacelle; 3, pylon; 4, foundation; 5, transformer [3]

A Wind Energy Conversion System (WECS), also known as Wind Turbines or Windmills, is a machine that converts the kinetic energy from the air to mechanical energy, which is also converted into electrical energy, using "the rotation of the impellers, driven by wind

power, which convert the kinetic energy of wind into mechanical energy of the impeller shaft, which drives the generator producing electrical energy" [3].

This thesis will focus on the use of this technology as intended for major electric power generation using 3MW WECS in a wind farm, ready to integrate into the grid.

A Wind Energy Conversion System (WECS) is composed of several parts (see fig. 2.1), such as the impellers (1), that harness the kinetic energy from the wind thanks to the shape of its airfoil, designed in way that creates lift and reduces drag by rotating over an axis that is connected through the hub to the nacelle (2), which is the part of the WECS that houses the electrical generation components. In MW WECS a heat exchanger is usually housed on the rear of the nacelle to dissipate the heat that the internal components of the nacelle produce. On top of the nacelle also, barometric equipment is placed. The nacelle sits on top of the pylon (3), a hollow tube manufactured in sections, and that usually can have a height between 60 and 140 m. The connection from the nacelle to the pylon is done on modern WECS with a motorized yaw bearing; this system allows the nacelle to change its orientation, to be in line with the wind direction, so that it can harness as much energy from the wind as possible. The pylon is anchored to the ground, typically in a concrete foundation (4) if it is onshore, and with a different system if the WECS is placed offshore. The energy produced by each individual WECS is then conducted through cables to a converter (5) that converts the DC current into AC and from there, the electricity is connected to the grid and transported where it is needed.

2.2 Internal parts of the nacelle

According to Y. Jiang [3], "the nacelle is the core component for a wind generating set and also the concentrated area of heat production in the operating process". The internal configuration of a nacelle is shown in Figure 2.2.

2.2.1 Gearbox

The gearbox connects the "slow shaft" moved by the impeller (20-30 rpm), to the rotor of the generator. The gearbox increases the speed of the shaft up to 1500-3000 rpm through different configurations (simple spur or planetary). In this speed-up process some of the kinetic energy is transformed to waste heat, due to friction. This heat is captured by
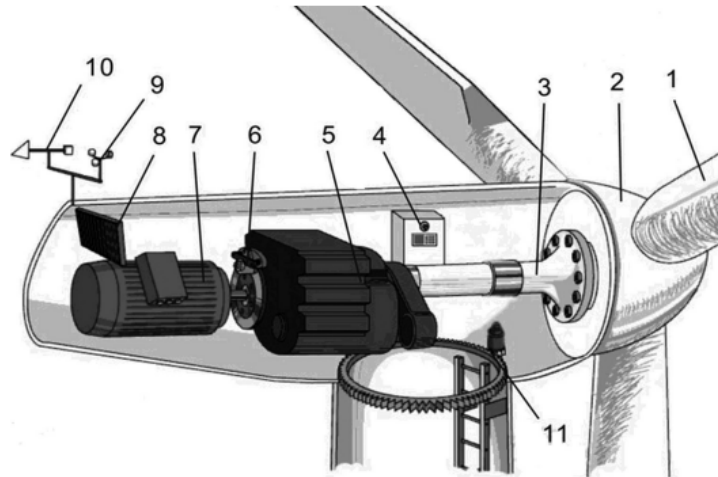
FIGURE 2.2: Nacelle internal parts: 1, impeller; 2, hub; 3, main shaft; 4, controller; 5, gearbox; 6, mechanical brake; 7, generator; 8, cooling system; 9, anemoscope; 10, wind vane; 11, yawing motor and yawing bearing [3]

the lubricating oil, which could become thinner and reduce its performance due to lower viscosity if the temperature becomes too high. Ultimately, this thinning of the lubricating oil could end up destroying the lubricating oil film, which would increase friction in the gears [12], causing an accident in the gearbox.

On the other hand, if the ambient temperature is under 0 ºC, the higher viscosity of the lubricating oil due to low temperatures, could also become a problem if the lubricating oil fails to splash onto the bearing surface. Normally, every large scale wind turbine gearbox contains a cooling and heating system for the lubricating oil [3].

2.2.2 Generator

The generator rotor, connected to the gearbox through the high-speed shaft, drives the generator rotating at high speed and cuts the magnetic lines of force, by which electric energy is obtained [12]. This also results in a loss of power, transformed into waste heat. The main sources of power loss are due to (1) copper losses, due to copper resistance in the winding copper wires of the generator; (2) iron loss, due to the rotation of the core hysteresis effect off eddy current, resulting in hysteresis loss and eddy current loss; (3) mechanical loss, since part of the energy is used to overcome friction [12]. All of these energy losses will ultimately be transformed into heat, distributed through the wind turbine nacelle.

Increasing the capacity of the generators linearly, increases the losses proportional to the cube of the linear increase in dimensions of the generator, thus decreasing the efficiency of the generator [12]. From this, it can be deducted that the enlargement of the unit capacity of wind turbines will depend in a big way, on the improvement of the cooling technology.

2.2.3 Control System

Due to the always changing nature of wind, auxiliary apparatus is installed to adjust the operating status promptly to ensure secure and stable operation. "The common system auxiliary apparatuses include: anemoscope, wind vane, yawing system, mechanical brake and thermometer. The anemoscope and the wind vane are used to detect immediate wind status; and the thermal sensor is responsible for monitoring the temperature changes in the generator and gearbox. When the operating status changes, the anemoscope, the wind vane and the thermal sensor will feed back the detected signal to the control system in the nacelle, then the input signal is diagnosed and processed by the control system and finally output to the yawing system and the mechanical brake, which changes the operating status of the wind turbine [...].
In addition, a frequency converter is equipped in the control system, which aims at converting the unstable frequency of wind turbine signal to suffice to the demands of parallel operation. Therefore, the control system is also called control converter. In the operation, the control system will produce a large amount of heat, which needs to be taken away timely" [3].

If the control inverter working environment temperature is increased by 10 $^{\circ}$C, it will reduce the control inverter life by half, while greatly increasing failure rate [12]. Therefore, it is important to keep the control system temperature under control.

2.3 Cooling system for WECS

The need of a cooling system inside the nacelle of a WECS comes as a consequence of the different waste heat loads of its internal components, mainly the gearbox, generator and control inverter, as explained above.

Wind turbine cooling technology can be divided in two main categories air or liquid cooling. Inside these categories the air cooling technology can be classified as natural, if the

air freely flow through the nacelle without any assistance, or forced air cooling, if fans are used to force the air through the nacelle ventilation system. The explanation given for the different wind turbine cooling technologies will be based on the chapter of the same name, from the book written by Yiang [3].

2.3.1 Air cooling

2.3.1.1 Natural air cooling

As early wind turbines had low power capacity, their heat production was also relatively small, and thus simply natural air flowing through the nacelle was enough to control the temperature inside the nacelle. This method is called natural air cooling and is still used today in WECS with a power capacity under 300 kW. As in this thesis, the focus is in larger MW wind turbines, this early adopted method is not of interest for the practical case of this paper.

2.3.1.2 Forced air cooling

The next iteration of WECS cooling method was the use of forced air cooling, in which fans installed in the air intakes of the nacelle introduced a forced flow of air inside the nacelle to dissipate the heat inside. "In a forced air cooling system, when the internal temperature of the nacelle exceeds a certain prescribed value, the control system will open a flap valve that connects the internal and external environment of the nacelle, and fans installed in the wind turbine are switched on, which produce a forced air blast to the components inside the nacelle" [3]. This can be utilized when the cooling needs are small, and when the external environment is at sufficient temperature difference with respect to the internal temperature of the nacelle, so that thermal energy can be exchanged from the internal components of the nacelle with the external environment air and the waste heat is dissipated; and second, if the outside flow of air is clean enough, since during the ventilation of the nacelle, severe corrosion on the internal parts is possibly caused by blown sand and rain, and this goes against the long-term secure operation of the wind generating set. This method proved itself useful as power capacity increased up to 750 kW, at that point the cooling needs become larger and thus a different method needs to be adopted. "As the power capacity of the wind generating set keeps increasing, merely

adopting forced air cooling method could not meet the cooling demands. Hence, liquid cooling systems are emerging" [3].

In the case of this thesis, since the power studied is bigger (3 MW) and the air conditions cannot be considered clean, due to dust and sand particles carried out by the wind in the studied desert locations, relaying only on forced air cooling to evacuate the heat of the WECS part is insufficient, and thus a comination between forced air and liquid cooling is necessary.

2.3.2   Liquid Cooling

For large and medium scale WECS with power over 750 kW, liquid cooling is usually installed to satisfy the cooling requirements of the internal parts of the nacelle.

As the liquid medium's concentration and specific heat capacity are much greater than that of the gaseous medium, the cooling system adopting liquid medium can obtain much larger cooling capability, as well as more compact system structure which can solve the problem of low cooling output and the enormous size of the air cooling system [3].
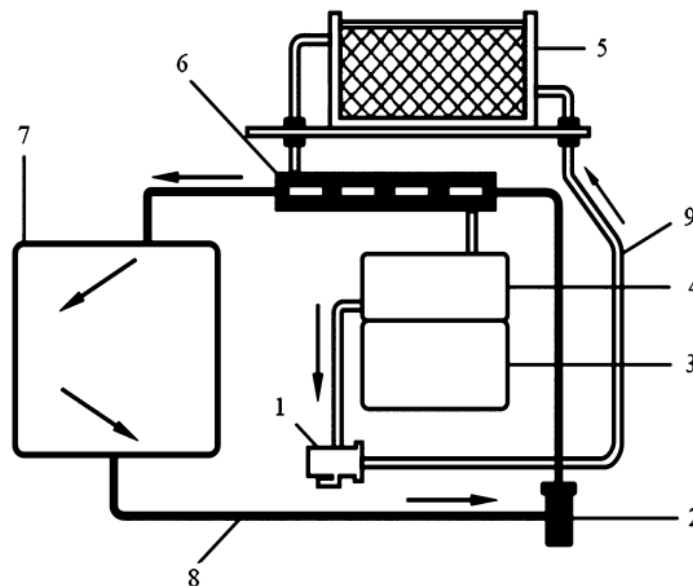
FIGURE 2.3: Liquid Cooling System scheme: 1, water pump; 2, oil pump; 3, generator; 4, generator heat exchanger; 5, external radiator; 6, oil cooler; 7, gearbox; 8, lubricating oil pipeline; 9, cooling medium pipeline [3]

In a liquid cooling system, "the cooling medium firstly flows through the oil cooler, exchanging heat with lubricating oil and taking away the heat produced by the gearbox.

Then it flows into the heat exchanger fixed around the stator winding, absorbing the heat produced by the generator. Finally, it will be pumped out and get cooled by an external radiator. The cooling water pump always stays in working mode to deliver internal heat to the external radiator through the cooling medium. And the lubricating oil pump can be controlled by the temperature sensor in the gearbox. When the oil temperature exceeds the rated value, the pump switches on, delivering the oil to the oil cooler outside the gearbox. When the heat production is comparatively large, a radiator outside the control converter can be installed to control its temperature rise through cooling medium taking away the heat in the same way of gearbox and generator. This is the case in large power capacity WECS, the gearbox, generator and control converter all produce comparatively large amount of heat, and cooling these components usually needs two independent sets of cooling system - one shared by the generator and control converter and other for the gearbox" [3].

In the design of the heat exchanger, due to relatively large difference of the cooling system operating loads in winter and summer, the summer operating mode is adopted as the design condition, while the heat transfer efficiency can be controlled through a bypassing method in winter.

A liquid cooling system has a more compact structure. Although it increases the cost of the heat exchanger, cooling medium and corresponding laying of connecting pipelines, it extremely enhances the cooling performance for the wind generating set, and thus facilitates the generating efficiency. Meanwhile, the design of the sealed nacelle prevents the invasion of wind, blown sand and rain, creating a good working surrounding for the wind turbine, which greatly extends the duration of the devices [12].

Although as it has been explained, most WECS over 3 MW use liquid cooling, for their primary cooling system, the secondary cooling system can still use natural or forced air cooling. There is where the air filtration system that this thesis pretends to improve is. In order to extract the heat from the primary cooling medium, air cooling with ambient air is used. In chapter 5, a case study specified for a 3 MW Vestas V112 will be explained. There an alternative filtration system for the secondary cooling system is designed and compared with mesh fiber filters.

Chapter 3

Dust Particles Filtration

3.1 Introduction

In this section, a model for particle measuring and collection is described, as well as a brief explanation of the different available devices for particle filtration and separation, that could be employed in the problematic this thesis is trying to solve. In that effort, a comparison between the typical method commonly used and the novelty proposal, that is between mesh-fiber filters and electrostatic precipitators, is presented.

3.2 Measuring and modelling particle separation

3.2.1 General concepts

When approaching the issue of measuring small particles in general, generalizations needs to be made, about the geometry of the particles, and the size of the particles, as they come in different shapes and sizes. That is why a model is needed, that gives an approximation of the quantity and size distribution of the particles in a given sample, as an exhaustive measure of each individual particle in a sample would be unnecessary and time consuming.

3.2.1.1 Particle size

As explained by N. M. Bojdo [4], no two individual particles are identical, which makes particle classification a troublesome affair, as a result of this, a mean or characteristic diameter is assumed and particles of different sizes as classified into size classes. To obtain a mean particle diameter, the concept of the *equivalent spherical diameter* is used, which as the name hints, assumes an equivalent volume of each particle as if it where a sphere, by relating some physical property of the particle to a sphere that would have equality on the same property, providing a characteristic size of each particle, so that a mean diameter can be used to model the whole sample
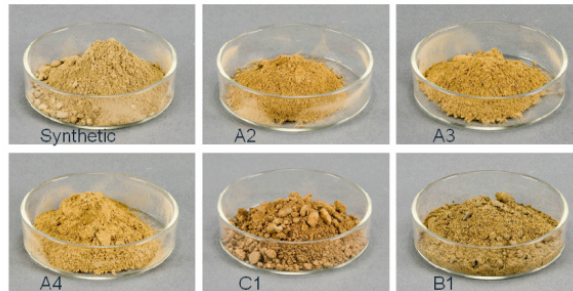
FIGURE 3.1: Photographs showing 6 sand samples from locations across the globe [4]
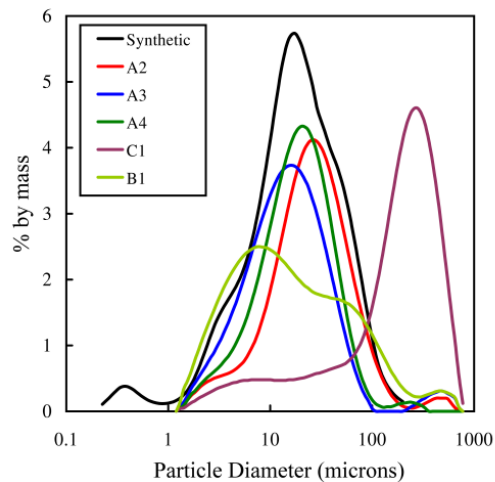
FIGURE 3.2: Particle diameter proportions as percentage by mass of six sand samples from locations across the globe [4]

Particles are grouped into size classes, each containing a range of diameters, so that the quantity and preponderance of a mean particle size is found in a given sample. For example, in figure 3.1, 6 sand samples from locations across the globe are presented and in figure 3.2, the corresponding size distribution diagrams, as it can be observed

in some samples a mean diameter can be clearly assumed, when the sample is fairly concentrated around one class (like in sample A2). However, when the distribution is more disperse (sample B1), a mean particle diameter could also be obtained, but it could be misleading when designing or selecting a particle filtration device. That's the reason why size class classification is important, not just to obtain a mean diameter, but because the distribution diagram can have valuable information.

In order to create the *particle size distribution* diagram, the first thing to do is to determine the number of classes that will be used, over an acceptable range that will cover the majority of the sample. Following the explanation of Parker [5], the border of a size class (i - 1) is denominated as x_i (x_1, x_2, ... x_n). The interval length of each class is termed as Δx_i, and the median of a size class as $d_{p,i}$ (fig. 3.3).
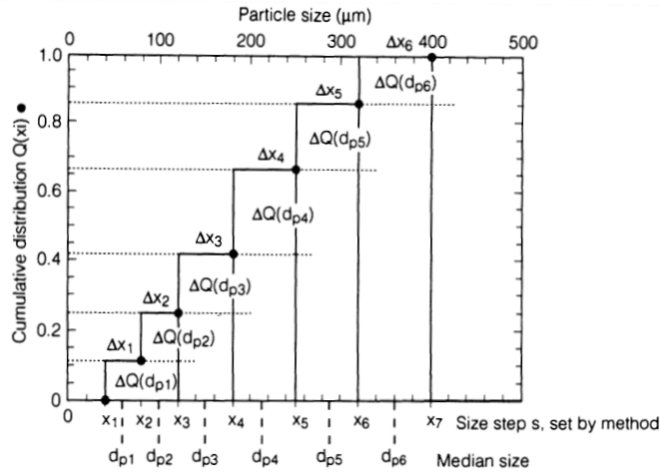
FIGURE 3.3: Particle size classification illustration [5]

After the determination of the classes by size, the relative mass is determined for each class. In particle size analysis, a cumulative mass distribution is often used, where x_i refers to the upper end of a size class. The relative mass of a class ΔQ is defined as equation 3.1 or 3.2 and the cumulative mass distribution Q by equation 3.3:

$$\Delta Q(d_{p,i}) = Q(x_{i+1}) - Q(x_i) \tag{3.1}$$

$$\Delta Q(d_{p,i}) = \frac{M(d_{p,i})}{M_{tot}} \tag{3.2}$$

$$Q(x_j) = \sum_{i=1}^{j-1} \Delta Q(d_{p,i}) \tag{3.3}$$

Where M for mass, Q stands for the quantity of mass, x for a size class and d for diameter. The subindex p refers to *particle* and i to the n-th value.

A function can be obtained (eq. 3.4) to determine the density distribution $q(d_{p,i})$, of a relative mass interval ΔQ:

$$q(d_{p,i}) = \frac{\Delta Q(d_{p,i})}{\Delta x_i} \tag{3.4}$$

3.2.1.2   Particle collection efficiency

Efficiency on a filtration process might seem simpler than it is, because the concept of *efficiency*, is widely known as the output over its input. In the case of filtration, it can be defined as how many of the particles that compose the fluid to be filtered are trapped by the filtration system, with respect to the initial amount. Or it can also be understood as what percentage of the particles of the initial fluid end up in the final fluid after the process of filtration.

Another component that could be taken into account, is how much energy is needed to reliably perform the separation and collection process, although that will not be discussed in this section. For example, mesh fiber filters are a passive system, but need of an external force, usually fans, to force the fluid through the pressure difference that the obstacle (mesh-fiber) on the duct poses. These fans consume energy. While ESPs create less of a pressure difference, they are an active system, and they need electrical energy in order to work.

This section will focus on a more extensive understanding of the first basic definition. That is, the efficiency of the device, as the percentage of particles that pass (or don't pass) through the duct, which can be considered *general efficiency*, but also what is defined as *grade efficiency* or fractional efficiency, which is the efficiency evaluated for each individual size class.
As it can be understood, some devices deal better with bigger particles, than they do with smaller ones and vice versa. Therefore, it is interesting to look at fractional efficiency curves, as they can give much more information about a filtration system than the overall efficiency of the device.

Two kinds of grade or fractional efficiency can be distinguished, based on the definition of efficiency. For a given particular size class, if the efficiency is measured as the collected coarse amount, related to the inlet particles, this is referred as grade efficiency $T(d_{p,i})$. When the efficiency is measured as the final particles that remain at the outlet, in relation

to the particles in the inlet, this is referred as fractional penetration $P(d_{p,i})$ [5]. These two magnitudes are inversely proportional and its sum will always equals one, $T+P$=1. As usually fractional efficiency is the most commonly used term, and the one the author of thesis will refer to when talking about grade efficiency.

$$T(d_{p,i}) = \frac{M_c(d_{p,i})}{M_e(d_{p,i})} = \frac{c_c(d_{p,i})}{c_e(d_{p,i})} \tag{3.5}$$

$$P(d_{p,i}) = \frac{M_f(d_{p,i})}{M_e(d_{p,i})} = \frac{c_f(d_{p,i})}{c_e(d_{p,i})} \tag{3.6}$$

If an integral balance is made for total particle collection, the result is a total efficiency E (eq. 3.7). The efficiency is generally defined as the mass balanced M, but it can also be expressed in mass concentrations c. The subindexes c, e, f stand for $collected$, $emitted$ and $final$ respectively.

$$E = \frac{M_c(d_{p,i})}{M_e(d_{p,i})} = \frac{M_e(d_{p,i}) - M_f(d_{p,i})}{M_e(d_{p,i})} = 1 - \frac{c_{f,tot}}{c_{e,tot}} \tag{3.7}$$

In order to calculate the grade efficiency, particle size distribution measurements need to be take. Combining equations (3.5) and (3.1) leads to a simpler relationship (eq. 3.8) for calculating grade efficiency from measured collected particles and inlet distribution:

$$T(d_{p,i}) = \frac{M_{c,tot} \cdot \Delta Q_c(d_{p,i})}{M_{e,tot} \cdot \Delta Q_e(d_{p,i})} \tag{3.8}$$

Using this relationship, the total mass efficiency can be deduced as equation 3.9 [5].

$$E = \sum_i T(d_{p,i}) \cdot \Delta Q_e(d_{p,i}) \tag{3.9}$$

3.3   Particle separation devices

There are different technologies that could perform the task of dust separation. In this section, a brief explanation of them, and whether they could be considered for the task of dust filtration in a WECS nacelle in the desert will be explained.

- **Mesh-fiber filters**, are the most common and conventional approach to air filtration. They consist of a series of layers of fabric, arranged in mesh structure and oriented perpendicular to the gas flow. They are composed by a natural or synthetic fiber, generally fiberglass. The particle removing mechanism of fiber-based filters is very simple and passive process in which particles in the air stream are removed when they attached to the fibers. The presence of the mesh in the path of the airflow results in a large pressure drop. Fiber-based filters create a pressure drop in order to capture the particles through their dense mesh, and require a fan so that the air flow needs to overcome this pressure drop. The denser the mesh the higher energy demand it needs from the fan so that the flow passes through the filter. Particles are unable to pass through fiberglass mesh because of three capturing mechanisms: impaction, interception and diffusion.
  Fiber-based filters are the most widely used filters because of their simple structures, easy installations, and low costs. However, fiber-based filters are unsuitable for highly dusty environments, as these conditions result in frequent maintenance or replacement [13]. In the case being study here, that would translate into a very high maintenance cost, as specialized labour would be needed.

- **Vortex Cyclone Separators** consist of a cylinder, in which the incoming airflow is forced to rotate at a high speed velocity. There is a rotating force which causes the dust particles carried by the flow to impact with the walls of the cylinder, thus, separation occurs. The separation efficiency is generally greater for bigger particles and lower for smaller particles, depending on the cut point. The cut point refers to a particle size in which the collection efficiency is of 50 %, increasing the efficiency above that particle size, and decreasing under it.
  Vortex separator are relatively big and complex machines. The separation efficiency is determined by the residence time of the particles in the cyclone and by the electric field strength. Its efficiency is not great for particles smaller than 1μm, and it decreases even more if the density of the fluid is smaller [14]. This can be expected to be the case in a high altitude desert environment, where it can be certain that

there are dust particles, but that the concentration of it on the air is not very high. Thus, this technology is discarded for this project.

- **Wet devices** e.g. wet scrubbers, consist of spraying small droplets of water to a polluted air flow in a closed space. The water will attach to the unwanted particles, and by gravity it will force them to go down, as a result the clean air, will go up, additionally passing through a series of filters, making sure the air is clean.
  Wet scrubber have a good grade efficiency for particles over 1 μm, but it is obvious that any device that relies on water for filtration is not appropriate for a WECS situated in the desert. Where, as it can be expected, water is a scare resource. Additionally, the performance of wet scubbers is worse than that of ESPs, regarding collection efficiency and power consumption [14] .

- **Electrostatic Precipitators** consist on a duct or series of ducts, in where an electrostatic field is created, and free moving electrons on this field impact with the dust particles flowing through it, leading them to precipitate on the walls of the duct. A more detailed explanation is given chapter 4.
  Although ESPs are expensive machines which demand a big load of energy, as the case studied in this thesis, proposes to utilize them on a energy generation machine, as it will be explained later, the author finds this a good alternative to mesh fiber filters.

3.4 The problematic

From the previous list, only conventional mesh-fiber filters, and ESP will be considered and will be compared from a performance and cost analysis in following chapters.
But first, in order to perform a proper comparison of this two air filtration devices, a brief explanation of why the conventional approach, i.e. mesh-fiber filters, should be replaced by the new proposed method, electrostatic precipitators is given here.

The reason to replace mesh-fiber filters for air filtration of nacelle WECS in the desert, is the environment. As it can be expected, in a dusty environment as the desert, the air can lift up and transport sand and dust from the ground level up to the hub height. The main problem with such a simple mechanism as mesh-based filters, is that dust can build up over time on the surface of the filters. As a consequence of this, there is an increasing pressure difference between the outside and the inside of the air inlet channel, that has to be overcome by the air flow necessary for the refrigeration of the WECS. This results

in a higher power demand from the fans to force the air inside, that require more energy to accomplish their task.

The dust builds up over time, this dust accumulation is referred as *dust cake* and can be dealt with in two ways, although it is never fully solved, as it always regenerates over time. The first one, is for an operary to periodically and manually clean them and replace them by another filter once the lifetime of the filter has finished. This approach, in the case being study here would result in very high labor costs. Because WECS, generally grouped in a 10 to 20 units windfarm, are placed in a remote location, far from cities to avoid visual and noise pollution; and because the operary would have to access them at hub height, which can be assumed to be at 100m. This access would be ideally climbing from the base of the WECS through the stairs inside the tower. But it is likely that the air inlet of the channel could only be accessible via the use of a crane or an elevator, repeated for each WECS. Additionally, the cost of transporting a crane to the windfarm location would have to be added, in case there is not one on the installation for maintenance.
Another viable solution for the elimination of the dust cake, is to install a pulse-jet, that is an intermittent stream of air, in the opposite direction of filtration, that could remove part of the dust from the filter when activated. The engine would use a compressor, to compress the air so that it can release it at a velocity high enough for the dust on the surface of the filter to detach from it and leave the channel through the inlet. This would not solve the overall problem as the dust cake will always periodically regenerate, due to the nature of the mesh-filter technology. Although less trips for the maintenance operator would be needed, they would be needed anyways, as eventually the filters can break and need replacement. This second solution, is not common, as it is relatively expensive and it adds complexity to a simple system, so it won't be considered in the comparison.

Depending on the frequency of replacement of the filters, the maintenance costs can add up to a very high amount, which is why in the author's perspective, it seems reasonable to consider replacing the cheap and simple air filtration mechanism for a more complex and expensive one. As an alternative, a more reliable solution, is needed, thus, the author proposes the installation of an electrostatic precipitator system, that create a much smaller pressure difference inside the duct, as the filtration does not use physical barrier, but rather it uses electrostatic force for the filtration, so the filtration efficiency is constant over time, as oppose to the mesh fiber filters. ESPs are in fact, more expensive, as the investment capital cost is substantially higher to that of a mesh-fiber filter, and as they require electrical energy for its operation, so not just a performance comparison is necessary, but also a cost analysis.

3.5 How to compare two different filtration systems?

3.5.1 Performance comparison

When comparing the performance of these two technologies, collection efficiency cannot be the only determinant factor. As a mesh-fiber filter with a very dense mesh, i.e. very small openings, could report a 100% efficiency for the unwanted particles, but the filter would clog too quickly, which would mean a higher maintenance cost because of particle accumulation. Additionally, the pressure drop created would be great, so the velocity of the fans would have to be greater, which would demand more energy.

The European standard that regulates air filtration is the EN779. This standard measures the average collection efficiency for particles of 0.4 μm of a synthetic AHSARE test dust (as they are the hardest to filter) at $3400\ m^3/h$. This standard only takes into account the ability to collect dust particles, and it does not pay attention to the energy that the filtration process consumes. Hence, to be able to compare the performance of fiber-based filters and electrostatic precipitator, is not very useful.

In fiber-based filters the pressure difference changes over time depending on the drift velocity and on the size of the dust cake. In ESPs it stays mostly constant over time. The collection efficiency of filters is an average one, because as explained at the beginning of the chapter, different efficiencies can exist for different particle size classes.

The energy consumed by an air filtration system with mesh-fiber filters, in most cases, corresponds to the energy consumed by its fan, as typical mesh-fiber filters are passive systems that do not require energy to function. The energy consumed by the fan E_{fan} in KWh can be calculated according to eq. 3.10, in where Q is the volume flow rate, t is the operation time in hours, Δp ,measured in Pa, is the pressure drop that the fan has to overcome and η_{system} is the efficiency of the fan.

$$E_{fan} = \frac{Q \cdot \Delta p \cdot t}{\eta_{system} \cdot 1000} \tag{3.10}$$

The efficiency of the fan is assumed to be 0.7, althought it can go as up as 85% in the best case, it is safer to assume 70% as it is a more typical value [15].
The operation time of a typical HVAC is usually assumed to be 6000 hours, which is 24 hours per day, 5 days per week, 50 weeks per year. In this thesis, as the ventilation system has to be adapted to a WECS, the operation time will be 2700 hours (30% of the total hours in a year), as wind production depends on wind availability. The capacity

factor, which refers to the hours of a year in which a WECS produces energy over its maximum theoretical production (24 hours a day, 365 days at rated power). The capacity factor for wind turbines ranges from $30 - 40$ %. For the calculations made in the case study (chapter 5) the most conservative capacity factor of 30% has been selected.

To calculate the total energy consumed by the ventilation system E_{Total} with the ESP, the energy consumed by the electrostatic precipitator has to be taken into account. Therefore, eq. 3.11 has been defined, which is the sum of the energy consumed by the fan E_{fan} over the operating time of a year, and the energy consumed by the precipitator E_{ESP} over the same period of time. In the case where there is a mesh-fiber filter, E_{Total} is equal to E_{fan}, as the filter does not consume any energy.

$$E_{Total} = E_{fan} + E_{ESP} \tag{3.11}$$

All this magnitudes will be used at end on the case study (chapter 5, section 5.5) where all the information of the specific desert location is listed.

3.5.2 Cost comparison

To perform a proper cost comparison, only the cost of the filters or the ESP, also called Capital Investment C_{CI} is not a good enough indicator. A cost-benefit analysis needs to be made to take into account all the indirect costs, that each filtration system has over the years.

The **capital investment costs** refers to the initial money needed to invest in a brand new system. This a direct cost. Electrostatic precipitators initial cost are several orders of magnitude more expensive than any mesh fiber-filter; while the **operation and maintenance cost** $C_{O\&M}$ (eq. 3.13) can vary depending on the operation cost, which is the energy consumed times the cost of energy C_{Energy} (see eq. 3.14); and the circumstances. Operation and maintenance are indirect costs. The cost of maintenance (see eq. 3.15) will be determined by the cost of replacing the parts needed, for the system to continue properly working over time, the cost of sending a technician to replace them C_{Labor} and the frequency with which which the filtration device has to be revised or replaced $f_{replacement}$. This frequency is estimated based on the lifetime of the filter L_{filter} (eq. 3.12).

$$f_{replacement} = \frac{1}{L_{filter}} \tag{3.12}$$

$$C_{O\&M} = C_O + C_M \tag{3.13}$$

$$C_O = E_{System} \cdot C_{Energy} \tag{3.14}$$

$$C_M = \frac{C_{labor} + C_{replacement}}{L_{filter}} \tag{3.15}$$

The lifetime of the filters will greatly depend on the operation time t and the flow rate needed for operation Q. Assuming that the filtration and ventilation system of the WECS only work when the WECS is generating energy, the operation time of the filtration system will be equal to that of the WECS.

The average operation time of any WECS, is the time of the year on which the WECS is active and generating electricity; depending on the specific location wind frequency and availability. The capacity factor however refers to the amount of energy a WECS produces over a year, in relation to the potential energy that it would have produced, if it had being working at rated power, all the hours of the year. As operation time can vary greatly depending on any specific place, in this thesis the operation time will be assumed to be the same as the capacity factor of a WECS, which is typically around 30 % of the total hours in a year. Thus, operation time is assumed to be 2700 h (rounded, 30 % of the total 8760 annual hours).

The **cost of energy** C_{energy} is assumed to be 0.040 €/kWh, as this value derives from an economical analysis of a 3 MW WECS [16], and it is independent of local electricity prices. This assumption is independent of the location of the WECS because it derives from the total cost of a WECS unit.

The sum of the capital investment cost C_{CI} and the operation and maintenance costs $C_{O\&M}$ over a established period of time, determines the **Total cost** C_{Total} (eq. 3.16).

$$C_{Total} = C_{CI} + C_{O\&M} \tag{3.16}$$

When all the parameters of the different costs are set, a comparison can be made. If all the costs are computed in a yearly basis, an initially more expensive alternative like the ESP may become, over the years, in a more cost-effective solution, if the operation and maintenance costs $C_{O\&M}$ are substantially lower than those of mesh-fiber filters.

The total cost C_{Total} of an ESP filtration system compared with a conventional mesh fiber-filter system, will be studied in chapter 5, when the parameters for the two systems applied in a desert climate WECS, are established.

Chapter 4

Electrostatic Precipitators

4.1 Introduction

In this chapter Electrostatic Precipitators (ESP) are described and why are proposed to substitute mesh-fiber filters is explained. This explanation, about what this technology is and how it works is extracted mostly from the Applied Electrostatic Precipitation book, edited by K. P. Parker [17], specifically [5].

4.1.1 What an ESP is

Electrostatic precipitators are particle filtration devices that using electromagnetism allow particle separation to happen on a free flowing fluid, without using any obstacles, such as mesh-fiber filter, that would increase the pressure difference, and increase the fans (that guide the flow) power demand, as more force would be needed to be applied, in order to overcome this pressure difference.

ESPs are typically used to trap dust, fume and mist. The size of the particles that are to be trapped depends on many conditions, such as flow velocity and residence time; voltage and current applied, and thus the strength of the electric field created; the temperature; the dust resistivity and the geometry of the ESP, mainly width and length.

ESPs can be classified in different categories. The most important ones are by steps, by usage, by geometry (flat or cylindrical duct) and also by the usage of water (wet or dry precipitators).

4.1.2 Where it is used

The first ESP patent dates back to the end of the XIXth century, where it was commercially first used to trap the fume of a lead smelting furnace. It was during the first part of the XXth century when it was developed and successfully applied to iron, cement and power plants. ESP allows air filtration for the reduction of pollution emission and it also allows to trap valuable scraps. From the 1950s until today ESPs have been mostly used to reduce pollutant emissions, in different industries such as chemical and power plants.

4.1.3 How it works

The main physical phenomenon that allows particle separation and collection without any obstacle is the electromagnetic force. To understand this, some level of familiarity with electric engineering and fluid dynamics is needed. Within this fields several forces explain the behavior that the particles follow, Van der Vaal's force, Maxwell's and others are present on the operation of an electrostatic precipitator. In section 4.2.3 the operation of the forces acting in an ESP is explained in detail.

The process of creating a charge that will guide the particle to its deposition, collection and removal, can be divided into 5 steps:

1. Generation of charge particles

2. Charging of the particles

3. Deflection and separation of the particles

4. Dust deposition

5. Dust removal

This 5 steps, can happen simultaneously, in what are called single-stage or one-stage ESPs. They can also be divided in two stages, where the generation of the charge and the charging of the particles, happen at one time, and the other three steps of dust separation, deposition and removal, happen afterwards. This is called a two-stage ESP.

This thesis will focus on one-stage ESPs.

4.1.4   Geometry/Architecture

In single stage precipitators, there are mainly two designs, which differ in the cross sectional area profile, in the orientation, and in the number of wires used. These two designs are *plate-type precipitators* and *tube-type precipitators*.

4.1.4.1   Tube-type precipitators

If the ESP has a circular profile, it is a tube, and therefore designated tube-type ESP. The walls that form the surface of this tube are electrically charged. Along the center of the tube, a wire runs parallel to the surface of the tube, creating an electrical field. This tube is oriented on the gravitational axis (see fig. 4.1.b), so that the gravity force leads the flow from the inlet to the outlet of the tube. As the walls are electrically charged the particles of the fluid are attracted to the surface of the tube. To remove the particles from the surface mechanical action can be used, for example, a brush, actuated as a piston can remove the dust layer of the walls, or other mechanism. Alternatively, a fluid can be flushed down the tube so that it cleans the walls of the tubes. The cleaning fluid is moved by gravity, precipitating the dust particles together with the fluid, to the outlet of the tube, so that they can be removed. The different method used for the removal of the particles, determines the classification of *wet* or *dry* ESPs.

4.1.4.2   Plate-type precipitators

When a rectangular profile is used, it is called plate-type ESP, a duct is formed by two parallel plates, which are electrically charged. This duct is oriented in the horizontal axis. In the middle of the duct created by these two plates there is a central row, with a series of wires, oriented perpendicular to the fluid and parallel to the plates (see fig. 4.1.a). These wires will charge the fluid particles flowing through the electrical field that these wires create. The plates are electrically charged with different polarity, so that when the particles of the fluid enter inside the field, created by the wires, the electrical force acts on the fluid particles attracting them to these plates, called collector plates. The particles deposited on the collector plates are removed by mechanical action.

The duct or series of ducts in a plate-type ESP can be divided into different sections of the same duct. These different sections can have different electrical fields inside of them. The reason for this is that, there are multiple wires, to which different electrical conditions

can be applied. This results in different fields, depending on the voltage applied, different electrical fields throughout the same duct can be created.

The size of the dust particles wanted to be filtered, will determine the electrical field applied in the section of the ESP. Different particle sizes inside the same fluid react differently to the same electrical field. Consequently, different particle sizes can be targeted, as the fluid carrying dust particles passes through a duct, which have different electrical fields inside of it.

Because of this characteristic of plate-type ESPs, in this project, only plate-type ESP will be considered, as the authors finds them more suitable for placing them on the nacelle of a WECS.
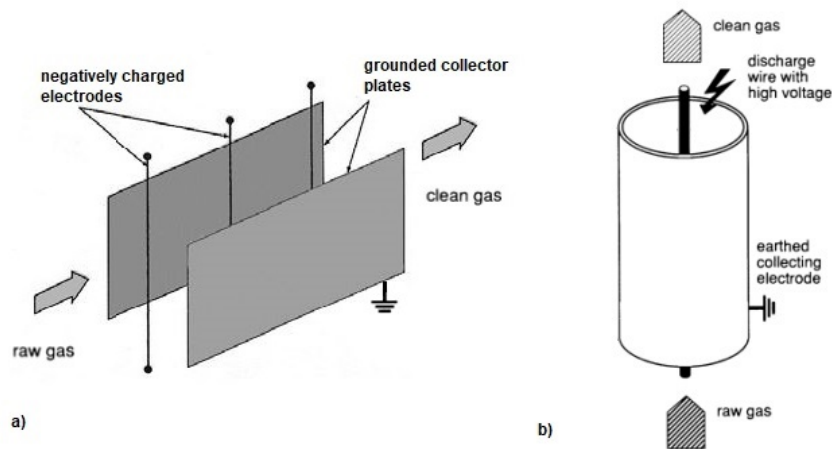
FIGURE 4.1: a)Plate-type electrostatic precipitator; b)Tube-type electrostatic precipitator [5]

4.2 Working Principles

In an effort to explain how an ESP works, the reader will be guided through the 5 steps previously mentioned in section 4.1.3. The complex concepts which describe and explain the behavior inside an ESP will be made as simple as possible, without losing the rigor that this thesis needs, so that a reader not familiar with this technology or field of study can understand this. Though the goal is to make accessible for any engineer to read, a ground in basic fluid dynamics and electrical engineering is still necessary to understand the physical principles governing this technology. If the reader wants a more academic and in-depth explanation of the working principles of an ESP, he can look that up in the source of this text, [5].

In order to understand how ESPs work, several concepts, magnitudes (real or dimensionless) and properties need to be explained. These will be defined as they come throughout the text, and designated with italics.

4.2.1 Generation of charge particles

4.2.1.1 Principles

An electrostatic precipitator is a filtration device. It is used to filtrate, that is separate some particles from others that jointly make up a fluid. This fluid is travelling along a duct, in which the process of filtration occurs. The fluid in question contains a series of unwanted particles. In the case being studied here, the fluid is air, and the unwanted particles are mostly dust and sand particles.

The phenomenon responsible for the filtration is the *electrostatic force*. It is related with the fundamental laws of physics and electromagnetism. The electrostatic force can be defined as the attractive or repulsive force between two electrically charged particles. Charged particles of the same polarity repel each other, and particles of different sign attract each other. By convention, the electrical current is usually denoted to flow from negative to positive sign polarity.

In an ESP, to have electrostatic force inside the duct, it has to be created. To do so, the collecting plates are assigned positive polarity, and are grounded; and the wires inside the duct are assigned negative polarity. These wire are *discharge electrodes*, which generate an electrical field, and create particles that are electrically charged.

These charged particles are free to move molecules (fig. 4.2), which have an electrical charge, in this case negative, and are called *charge carriers*. Charge carriers can either be positive or negative (i.e ions or electrons) depending on the polarity assigned to the elements of the ESP.
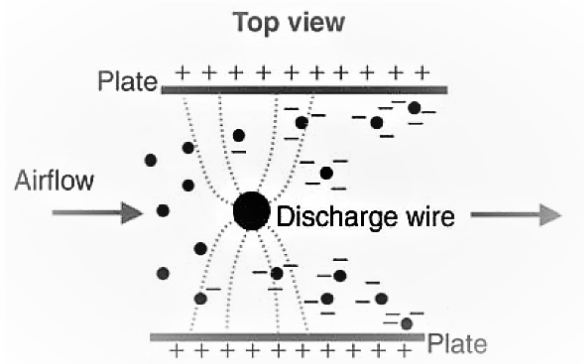
FIGURE 4.2: Corona discharge [6]

The principle that produces charge carriers is known as *corona discharge*. It is a release of electricity, as a result of the ionization of a fluid, in this case air, surrounding a conductor that is electrically charged. A corona will occur when the strength of the electric field around a conductor is high enough to form a conductive region, but not high enough to cause electrical breakdown or arcing to nearby objects. Usually, spontaneous corona discharges occur naturally in high-voltage systems, and are unwanted, as they are a waste of energy, but here they are controlled and essential for the working of the ESP. Corona discharges produce a crackling noise and emit a weak blue glow, as highly activated molecules emit photons.

To generate a corona discharge, that produces a quantity of charge carriers high enough to intercept the dust particles and lead them to the collector plates, a critical electrical field strength has to be overcome, usually of the order of $1 \cdot 10^5 - 5 \cdot 10^5 \ V/m$. To do this, high voltage is applied on the electrodes of the ESP, "when the applied voltage exceeds a distinct value, [called] *corona on-set voltage*, an electrical current between the two electrodes can be measured indicating a corona discharge" [5].
If the applied voltage is low enough and does not reach corona on-set, the ESP won't work because there is no corona discharge and thus no charge carriers will be produced. However, there is also an upper limit, if the voltage is too high, *spark-over* will occur. A spark over marks the electrical breakdown of the gas, it means that the discharge begins to pass straight through the gas and the ESP fails to work, since the charge carriers fail to use the charge to move the gas particles.

As referred by many authors [5, 18], the discharge electrode can be operated either on negative or positive polarity, but it is commonly accepted that negative polarity can be operated at higher voltages, since for certain geometries, the corona initiation voltage and the electrical breakdown of the gas occur at higher voltages for negative energization than for positive.

4.2.1.2 Electrostatic Field

Corona initiation field strength

It can be stated that different fluids, with different composition, will require different conditions, for the ESP to work properly. For this reason, the first electrical magnitude to set is the required electrical field strength to start the corona discharge, and thus the filtration process.

The charge carriers travelling toward the collecting plate will impact (collide) with the dust particles of the flow, the average distance travelled between collisions is called *mean free path*. This magnitude depends on the density of the gas, as denser gases will have a shorter mean free path as the provability of a collision is larger than in a lower density gas, where the concentration is smaller.

A function of gas density will therefore be, the required electric field strength to initiate the corona discharge. This magnitude is called *corona initiation field strength* E_0. The electrical field inside the ESP, is generated by the electrodes, which generally can have different electrical conditions, because as explained before, as the fluid advances through the duct, its composition changes, and therefore the required electrical conditions to filter it. Also, there are many complex designs for the electrodes, although generally assumed as a simple wire, in reality they are not simple rods. For this reason, as stated by Parker [5], the calculations are very complex and a pure theoretical description is still missing. There is however, a semi-empirical approach proposed by Peek to determine the corona initiation field strength E_0. In this approach, the initial field strength E_0 (eq. 4.1) is expressed as a function of the relative gas density δ (eq. 4.2), the discharge wire radius r_{SE} and two empirical constants (A,B) characterizing the gas and corona polarity.

$$E_0 = A\delta + B\sqrt{\frac{\delta}{r_{SE}}} \tag{4.1}$$

$$\delta = \frac{\rho_1}{\rho_2} = \frac{p_2}{p_1} \cdot \frac{T_1}{T_2} \tag{4.2}$$

Where constants $A = 3.2 \cdot 10^6 \ V/m$ and $B = 9 \cdot 10^4 \ V/m^{1/2}$. And temperature T and pressure p are usually related to normal conditions ($T_0 = T_1 = 273K$, $p_0 = p_1 = 1bar$). From empirical data it can be deduced that, in general, the corona field strength depends on the gas composition and the electrode design (mostly its radius), and an increase of the wire radius r_{SE} leads to a decrease in corona initiation electrical field strength. Although only up to a point, in radii larger than 1 mm, where that decrease seems to stop.

Electrical field distribution

The electric field generated in the ESP is inhomogeneous, this means that is not equally distributed along the duct space. The distribution of the field depends on the geometry of the precipitator, it can be divided into two clearly distinct zones, depending electrical field strength. These two regions are called *Active* and *Passive* zones (fig. 4.3). The distribution of the field and the different zones can be clearly distinguished in fig. 4.4, and this is due to the geometry of the discharge wire, generally curved surfaces, which results in high electrical field strength close to the wire, and an exponential decrease further from it. For this reason, wire-to-plate spacing (denoted by s) is a crucial parameter of the design of the ESP for the electrical field.

The active zone is where the ionization process occurs. It is very small compared to the passive zone, where the electric field is not high enough to generate the electrons, but in the passive zone is where the electrons attach themselves to the dust particles, deflecting them towards the collector plates. Thus the passive zone is where the separation process occurs. The distribution of the electrical field in the duct, governs the distribution of the current on the collecting plates, the charging of the particles and their migration.
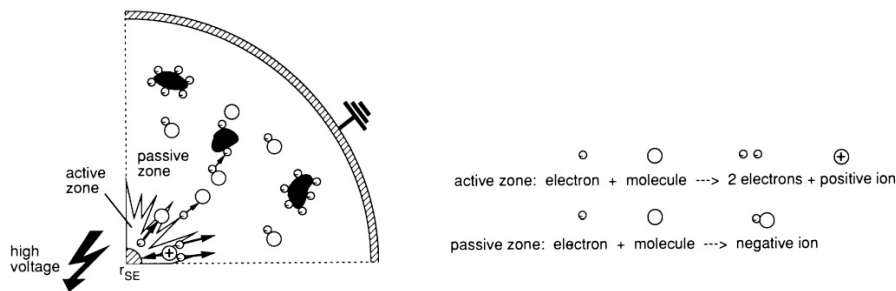
FIGURE 4.3: Active and passive zones representation of a tubular-type ESP [5]

As soon as the the electric field strength E overcomes the corona initiation value E_0, ions are produced. This electrical field strength, is a local function of the wire. The electrical field distribution depends as said before on the geometry and also on the electrical state of the precipitator. Simplifying it, the electrical state can be described by an electrical field

strength which is equal to the applied voltage over the wire-to-plate distance s (eq. 4.3). As this is a simplification, it gives a rough approximation of the real value (typically around $3.5 - 4\ kV/cm$). This estimated electrical field strength is called *pseudohomogeneous* electrical field strength E_{ps}.

$$E_{ps} = \frac{U}{s} \tag{4.3}$$

For plate-type ESPs, the electric field distribution can be broken up into its vector components, being the E_y component, the one responsible for the transport towards the collecting plates. As it can be expected, it is very high close to the wires and reaches a constant level a couple orders of magnitude smaller than the one reached around the wires, near the collectors wall region. Between the wires it decreases close to zero. A representation under dimensionless form is presented, being x' x/s and y' y/s for a plate-type precipitator with 5 discharge wires (see fig. 4.4).
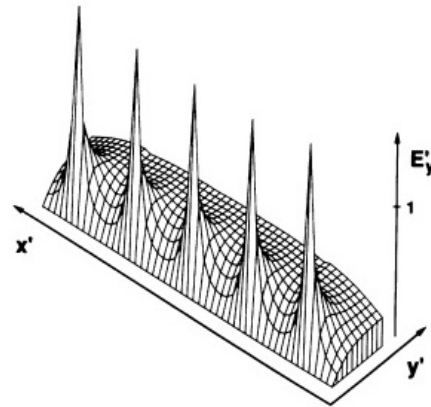
FIGURE 4.4: Three-dimensional plot of the spatial distribution of the E_y-component [5]

To obtain the real electrical field strength an iterative process needs to be done, to solve Poisson's equation and the equation of continuity of electrical charge, so that the distribution of the gas ions is known. However, such detailed computations are restricted to simple electrode geometries. For practical applications, simpler approaches, such as neglecting space charge or assuming a homogeneously distributed charge, are often preferred. In the model that will be explained later (Deutsch Model) the assumption of homogeneous field is made.

4.2.1.3   Voltage and Current

Corona on-set voltage

Having the initiation filed strength needed established, from this, the required voltage can be obtained. As known, from electricity fundamental laws, the electrical field depends on the voltage and the current. The electrical field is proportional to the voltage, and the voltage is proportional to the current via Ohm's law.

The *corona on-set voltage* V_0 depends on the precipitator's geometry, and on the design of the discharge and collecting electrodes. The geometry of a plate-type ESP can be described by several characteristic lengths (see fig. 4.5). As most things on engineering there are trade-offs in design, if the wire-to-wire spacing ($2c$) is too short, this will interfere in the corona discharge. However, a very wide wire-to-wire distance will result in an inefficient particle collection, although lower corona voltage will be needed in that case, but the electrical field in the space between them will decrease, and therefore the particle collection efficiency of the ESP. For plate-type ESPs, the corona-onset voltage is regulated
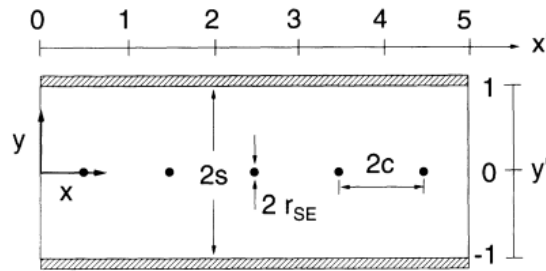
FIGURE 4.5: Plate-type nomenclature [5]

by the discharge wire radius r_{SE}, and also by an important characteristic length ratio d, which is a function of the wire-to-wire space ($2c$) and the wire-to-plate distance (s). The corona onset voltage for plate-type ESPs is given by equation 4.4.

$$V_0 = E_0(\delta, r_{SE}) \cdot r_{SE} \cdot ln \ \frac{d(s, \ 2c)}{r_{SE}} \tag{4.4}$$

$$\frac{d}{2c} = \frac{4}{\pi} \cdot \frac{s}{2c} \qquad\qquad \text{for } s/2c < 0.3 \tag{4.5a}$$

$$\frac{d}{2c} = 0.18 \cdot exp(2.96 \cdot \frac{s}{2c}) \qquad\qquad \text{for } 0.3 < s/2c < 1.0 \tag{4.5b}$$

$$\frac{d}{2c} = \frac{1}{2\pi} \cdot exp(\pi \cdot \frac{s}{2c}) \qquad\qquad \text{for } 1.0 < s/2c \tag{4.5c}$$

Depending on the wire-to-plate to wire-to-wire ratio ($s/2c$), the values for the characteristic length d can be calculated according to the different relationships (4.5a, 4.5b, 4.5c). Wire-plate spacings (s) larger than the wire-to-wire distance ($2c$) progressively dominate the characteristic length d. An increase in d will yield a higher corona onset voltage, which can be lowered by increasing the radius of the discharge wire r_{SE}.

Current

As just seen on the previous section, the voltage depends on the geometry, and is determined by the electrical field strength needed, for the ESP to work properly.

The current is related to the voltage by Ohm's law ($V = R \cdot I$). And it is proportional to the voltage, depending on the resistance, on this case the resistance is not constant, as it changes with time. That is because, as said before, different voltages work differently on the same sample size, and because concentration of dust in the fluid can change according to position along the duct, and because as the air is entering from the ambient, an uncontrolled environment, it can be expected that the concentration varies according to the climate conditions of the environment.

The electrical current, fundamentally, is a flow of electric charge. Electrons passing through a wire or ions in an ionized gas, as in this case. It is important to control the current, because in an ESP, it regulates the velocity of the charge carriers, which are ions. As it will be explained later, this charge carriers will collide with the dust particles following the current, leading the dust particles to the collecting plates. For now, it is important to note that, the drift velocity of the gas ions is proportional to the electrical field applied. And that this relationship is described by the constant of proportionality called *electric mobility of gas ions* b_i.

Ion mobility (eq. 4.6) is inversely proportional to the relative gas density (see eq. 4.2), and depends on pressure and temperature. This equation can be particularized for air under normal conditions $b(p_0, T_0) = 2 \cdot 10^{-4} m^2 / Vs$. For typical electrical field strengths in ESP, (e.g. $1 \cdot 10^5 - 5 \cdot 10^5 \ V/m$), the gas ion's velocity ranges between 20 and $100 \ m/s$.

$$b(p, T) = \frac{b(p_0, \ T_0)}{\delta} \tag{4.6}$$

As the current is a flow of electric charge, the electric current flux j is the rate of charge passing through a certain space, that is the charge per unit time and per unit area. Therefore the current depends on the area. Typical characteristic value of an ESP current flux are around $0.10 - 0.50 \ mA/m^2$.

The characteristic length that characterizes the functioning of the ESP electrical conditions in the duct cross sectional area, is the plate-to-plate spacing $(2s)$. The ratio of wire-to-plate distance (s) over the wire-to-wire spacing $(2c)$, d is generally equal to 1. This is because it is the most efficient design, as when the distance from the wire to the plate, and the distance from one one wire to the other is the same, the largest current is produced at this rate.

This is shown in figure 4.6, where for a typical ESP different wire-to-wire spacings are tested for the conditions of "half-duct spacing of $s = 200mm$, a wire radius $r_{SE} = 1.0mm$, an applied voltage of $40\ kV$ and an ion mobility of $3.1 \cdot 10^{-4}\ m^2/Vs$. If the wire-to-wire distance $2c$ is very small, the corona will be completely suppressed" [5].
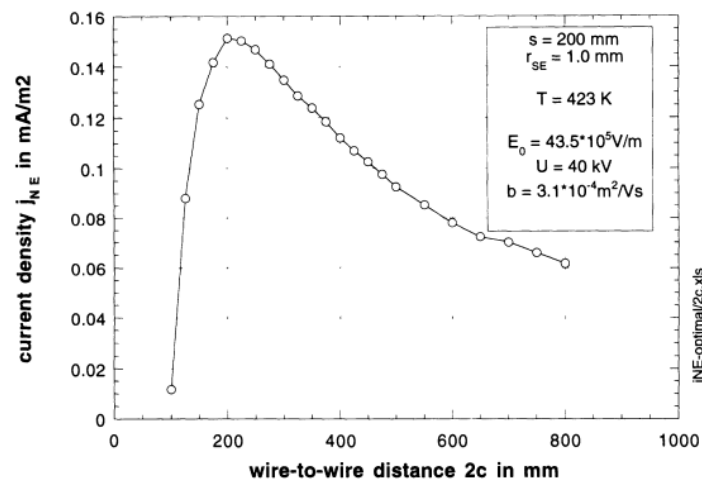
FIGURE 4.6: Current density as a function of wire-to-wire spacing for given duct widths and given wire radius [5]

4.2.2 Charging of the particles

4.2.2.1 Charging process

How do dust particles, that have neutral electrical charge become ionized? This is what this section will explain. But first, the gas that carries these particles has to be described.

There is a gas, air, which has solid particles in it flowing through the ESP duct. These solid particles are the dust particles dispersed in the air, and are said to have Brownian motion.

Brownian motion is the random movement of particles in a fluid, resulting from their collision with the fast-moving molecules inside the fluid [19]. Brownian motion, was discovered in 1877 by Robert Brown, a botanist, while he was studying microscopic life, he noticed little particles of plant pollens jiggling around in the liquid he was looking at in the microscope. The complex mechanics of this motion were later explained by Albert Einstein in 1905. The many body interactions that yield the Brownian pattern cannot be solved by a model accounting for every involved molecule. In consequence, only probabilistic models applied to molecular populations can be employed to describe it.

The charging of the dust particles flowing through the duct can be separated into two regions, depending on two physical phenomena, which broadly correlate with the size of the particles. That is, that for particles >1 μm there is a field charging region, for this, the presence of an electric field, which drives the free movable charge carriers, is necessary. For particles <0.1 μm, there is a diffusing charging region, in which the electrical field is not the driving force. But rather temperature is what causes the random movement of gas ions (according to Brownian motion), that intersect with each other and some particles which results in the charging of these smaller particles.

Although, actually particles of all sizes experience both phenomena simultaneously, the calculation of how the two phenomena combine is hard to measure. Also, diffusion models commonly underestimate the impact that this mechanism have on particle charging. A possible explanation can be agglomeration, when the fluid particle concentration is high enough.

One way to characterize the charging evolution of a dust particle is the *Cochet analytic equation* (eq. 4.7). Cochet's model shows that for particles ≥ 0.1 μm, the charge after a long time (saturation charge) is proportional to surface area and it increases linearly with electrical field strength. The saturation charge Q_p^∞ (eq. 4.9) will depend on the electrical

field strength E, the particle size d_p and the permittivity of the particle material ε_r.

If a homogeneous electric field is considered (ideal case), the dynamic charging behavior of particle size is independent of particle size, and it behaves according to the following equations:

$$Q_p(t) = Q_p^\infty \cdot \frac{t}{t + \tau_Q} \tag{4.7}$$

$$\tau_Q = \frac{4\,\varepsilon_0}{c_Q\,b} \simeq \frac{4\,\varepsilon_0}{j_{NE}/E} \tag{4.8}$$

$$Q_p^\infty = [(1 + 2\lambda/d_p)^2 + (\frac{2}{1 + 2\lambda/d_p}).(\frac{\varepsilon_r - 1}{\varepsilon_r + 2})] \cdot \pi\,\varepsilon_0\,d_p^2\,E \tag{4.9}$$

Where τ_Q (eq. 4.8) is a time constant specified with the electrical conditions present at each moment, c_Q is the concentration of gas ions, which can be expressed in terms of current density j_{NE}, mobility and electrical field E.

In ESPs, for typical electrical states, τ_Q has values $\leq 10\,ms$, and under typical electrical conditions particles will reach about 90 % of their saturation charge Q_p^∞ within 10 ms.

4.2.2.2 Particle Migration

Once, how particles get charge has been explained, it is convenient to explain how this affects the particles, moving down the ESP duct.

The particles of the fluid travelling through the duct, experience different forces acting on them, which explain their migration along the duct. The sum of all forces acting on the particles of the fluid, following Newton's first law, has to be zero $F_t + F_{el} + F_w = 0$. These forces are:

- The momentum force $\vec{F_t} = -\,m \cdot \vec{a}$

- The electrical force $\vec{F_{el}} = Q_p \cdot \vec{E}$

- The drag force $\vec{F_w} = c_w(Re) \cdot A_{pr} \cdot \frac{\rho_f}{2} \cdot v_{rel} \cdot \vec{v_{rel}}$

Where ρ_f is the density of the fluid and c_w is the drag coefficient, which is given by equation 4.11 and depends on the Reynolds Number (Re), which for typical ESP conditions and particles smaller than 20 μm is very low ($Re<<1$).

$$Re_p = \frac{d_p \cdot |\vec{v_{rel}}|}{v} = \frac{d_p \cdot |\vec{v} - \vec{w}|}{v} \tag{4.10}$$

$$c_w = \frac{24}{Re_p} \tag{4.11}$$

Regarding the drag force, the equation that characterizes the motion of a charged sphere in an electrical field E is equation 4.12. For this differential equation to hold, several assumptions have to be made: the fluid to have no component towards the collecting plate, that means, that it is flowing parallel to the collecting plate; and that the particles have reach saturation charge.

$$\frac{dw}{dt} + \frac{3\pi\eta d_p}{m(Cu)}\, w = \frac{Q_p^{\infty}}{m}\, E \tag{4.12}$$

$$w\left(t\right) = w_{th} \cdot \left(1 - exp\left(-\frac{t}{\tau_p}\right)\right) \tag{4.13}$$

Where w represents the drift velocity (average velocity of the electrons) and Cu is the Cunningham factor, a correction factor for the drag force. This factor is used when the particle size reaches a region where the fluid loses its continuum characteristic, not explained here, due to its complexity.

A new magnitude is introduced, *theoretical migration velocity* w_{th} (eq. 4.14), which represents the average steady state velocity of the particles. This magnitude is strongly influenced by the electrical field (see fig. 4.7). The theoretical migration velocity depends also on size, it decreases linearly with particle size until it reaches a minimum at 0.35 μm, where the behaviour changes and start increasing.

$$w_{th} = \frac{Q_p^{\infty}}{3\pi\eta d_p}\left(\cdot Cu\right) \tag{4.14}$$

Another magnitude, *relaxation time* τ_p (eq. 4.15), measures the time particles need inside the electrical field to reach steady state velocity. Although it doesn't depend on electrical field strength, this magnitude increases linearly with particle size, which means that the larger the particle, the more time it will need to reach steady state velocity, or it will have reached in a lower steady state velocity in the same time. For example, "particles < 6 μm after 1 ms, have already reached steady state velocity, while a 10 μm particle has reached 80%, and a 20 μm particle about 30 % in the same time" [5].

$$\tau_p = \frac{m_p\left(\cdot Cu\right)}{3\pi\eta\, d_p} = \frac{\rho_p \cdot d_p{}^2}{18\eta}\left(\cdot Cu\right) \tag{4.15}$$
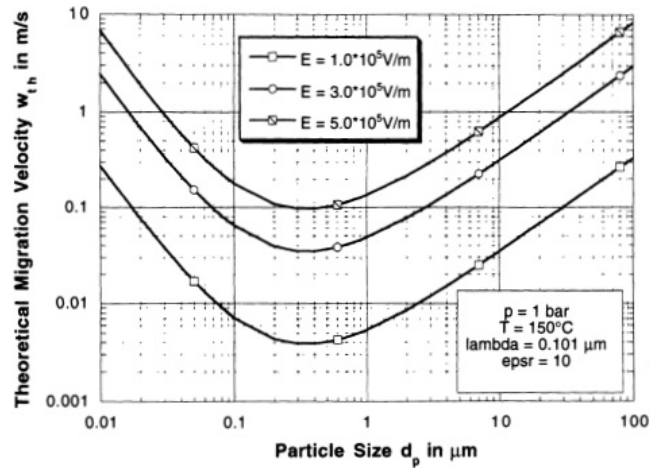
FIGURE 4.7: Plot of theoretical migration velocity as a function of particle size for three different electric field strengths [5]

It is worth mentioning that very fine particles under 0.1 μm, don't behave the same way, because as explained in section 4.2.2.1, they are more influenced by diffusion than by the electrical field charging them, thus, very fine particles need a higher residence time and therefore a lower velocity than particles over 1 μm.

4.2.3 Deflection and separation the particle

In the previous sections (4.2.1, 4.2.2) how the charge is produced and how the particles of the fluid travelling along the ESP duct are charged has been explained. In this section, how dust particles deflect, that is, a change in the angle of movement, and thus separate from the initial fluid into the collector plates is explained.

To do this, it is necessary to understand how the dust particles that compose the fluid move inside the duct under electrostatic excitation. Or at least, as knowing the position and trajectory of thousands of micro-particles might be too daring, it is fair to propose some assumptions, and assert an accurate model, that helps realize this purpose.
The model used in electrostatic precipitators, is the *Deutsch Model*, a variation over the *Laminar Model* with a certain level of turbulence. Thus the author of this thesis considers that explaining superficially both could help a reader not proficient in fluid dynamics (as the author himself is not) to at least picture how the fluid behaves inside an ESP. Therefore, the assumptions needed and the Laminar Model will be discussed first, to establish the basis for understanding the Deutsch model.

4.2.3.1   Assumptions

As most models, the Deutsch model is not perfect, it is an ideal model, and ideal models need corresponding idealized conditions. So assumptions are needed. In electrostatic precipitation, all standard models refer to the ideal precipitation process, that means, that all negative influences are known and ignored. The assumptions that have to be made in an ESP so that a model can be employed are the neglection of:

- Back-corona of the dust layer

- Re-entrainment of precipitation dust

- Field bypassing (also referred as sneakage)

4.2.3.2   Laminar Model

On fluid dynamics the world *laminar* refers to the state of a fluid that flows in parallel layers, without intermixing between the adjacent layers, this tends to occurs generally at low velocities (in particular when the Reynolds number is under a certain number). "In laminar flow, the motion of the particles of the fluid is very orderly with particles close to a solid surface moving in straight lines parallel to that surface" [20].

In the case being studied here (ESPs) it refers to the lack of any driving force that moves the particles in a different direction to the one of the gas flow or the electrical force, that moves the particles according to the electrical field. This translates in no remixing force arising from turbulence [5]. Under this model, particles are assumed to be fully charged, and the electrical field to be homogeneous. In a laminar model the grade efficiency is determined by straight particle trajectories. That can be expressed as the ratio of the mean gas residence time in the precipitation zone, to the time a particle of size d_p needs to travel the distance between the electrode and the plate (t_s) :

$$T(d_p) = \frac{w_{th}(d_p, E) L_{NE}}{v_0 \, s} = \frac{t_{res}}{t_s(d_p, E)} \tag{4.16}$$
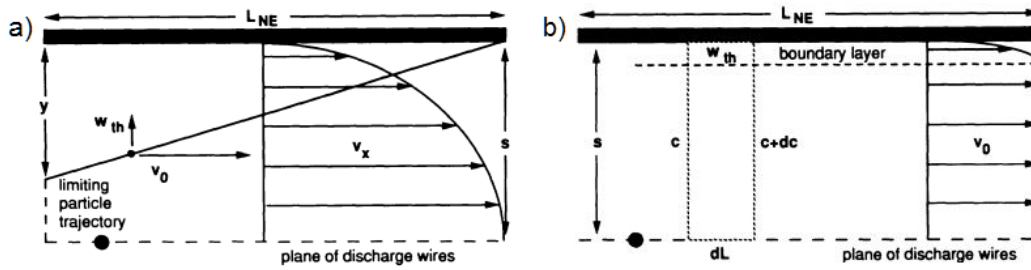
FIGURE 4.8: Sketch of the (a) Laminar Model and the (b) Deutsch Model [5]

4.2.3.3 Deutsch Model

The Deutsch Model was design for ESPs in 1922 by Walter Deutsch and it is still today, widely used to predict the flow behaviour in ESPs. This model is not laminar, it assumes an infinite remixing force, e.g. caused by turbulence. This remixing force redistributes homogeneously the remaining particles in the duct at each location. It also assumes that the particles in the downstream direction have the mean velocity of the fluid, are fully charged and migrate in a homogeneous electrical field [5].

In real ESPs the model predicts fairly accurately the grade efficiency of particle collection. It is very accurate for particles $> 10 \ \mu m$, fairly accurate for particles between 1 and $10 \ \mu m$, and it fails to predict the grade efficiency collection for submicron particles.

In figure 4.9, the experimental result and different models, like laminar or Deutsch and other PTMs, are compared for a lab scale ESP with the following conditions: $v = 1.0 \ m/s$, $s = 100 \ mm$, $L = 5s$ and $U = 50 \ kV$. PTM stands for Particle Tracking Model, which are computer simulations assuming homogeneous or inhomogenous electrical field conditions. It is interesting to note that all models underpredicts the collection efficiency for
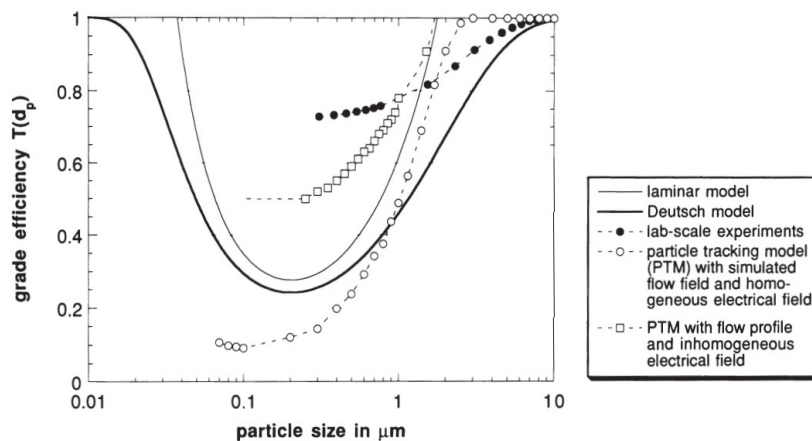
FIGURE 4.9: Grade efficiencies of different models together with experimental values [5]

particles $< 1 \ \mu m$. The better performance of these particles could be due to fine particle being better transported than assumed, or due to the assumption of homogeneous electrical field, when as explained before, the electrical field is in fact inhomogeneous. The particle collection over the duct length is not homogeneously distributed, even under idealized conditions, dust free zones can be observed on the collectors.

The main interest for the Deutsch Model, it is for its ability to predict the efficiency of the precipitators, as discussed above, it is accurate enough and wide spread in the available literature, so that it will be the one used in this thesis.

Grade Efficiency. The Deutsch model is described by several equations, which describe the efficiency of the collection process, from the study of the concentration of dust particles on the fluid. In particular, the grade efficiency T_{d_p}, previously explained in section 3.2.1.2. It can be obtained studying the concentration a control volume on a plate-type precipitator (see fig. 4.8), resulting in the differential equation 4.17. Integrating this equation, the concentration of particles as a function of the downstream location L is obtained (eq. 4.18).

$$\frac{dc(d_p)}{c(L, d_p)} = -\frac{w_{th}(d_p)}{v_0 \ s} \cdot dL \tag{4.17}$$

$$c(L, d_p) = c(0, d_p) \cdot exp\left\{ -\frac{w_{th}(d_p, E) \ L}{v_0 \ s} \right\} \tag{4.18}$$

Transforming the concentration into grade efficiency for plate-type precipitators, eq. 4.19 is obtained. Although, a general formulation can also be obtained, whether the precipitator is plate-type or tube-type, when the total collecting area and the total flow rate are used (eq. 4.20).

$$T(d_p) = 1 - exp\left\{ -\frac{w_{th}(d_p, E) \ L_{NE}}{v_0 \ s} \right\} \tag{4.19}$$

$$T(d_p) = 1 - exp\left\{ -w_{th}(d_p, E) \ \frac{A_{NE}}{\dot{V}} \right\} \tag{4.20}$$

The exponent term of either equation 4.19 or 4.20, is referred as the *Deutsch number*. The Deutsch number (De) is inversely proportional to the penetration, which is the inverse of the grade efficiency. Thus, the the grade efficiency is directly proportional to the Deutsch number. The Deutsch number can be interpreted as a dimensionless residence time (eq. 4.22).

$$T(d_p) = 1 - exp\left\{ -\ De\ (d_p; E, v_0) \right\} \tag{4.21}$$

$$De = \frac{w_{th}(d_p; E)}{s} \cdot \frac{L_{NE}}{v_0} = \frac{t_{res}(v_0; L_{NE})}{t_{drift}(d_p; E; s)} \tag{4.22}$$

The strong influence on the grade efficiency (and therefore on the Deutsch number) of the electrical field strength was demonstrated, in an experiment for a plate-type precipitator of 5 m length, where the minimum grade efficiency around 0.35 μm is shifted from 5% up to 70%, by increasing the field from 1.0 to 5.0 $\cdot$ 10^5 V/m [5].
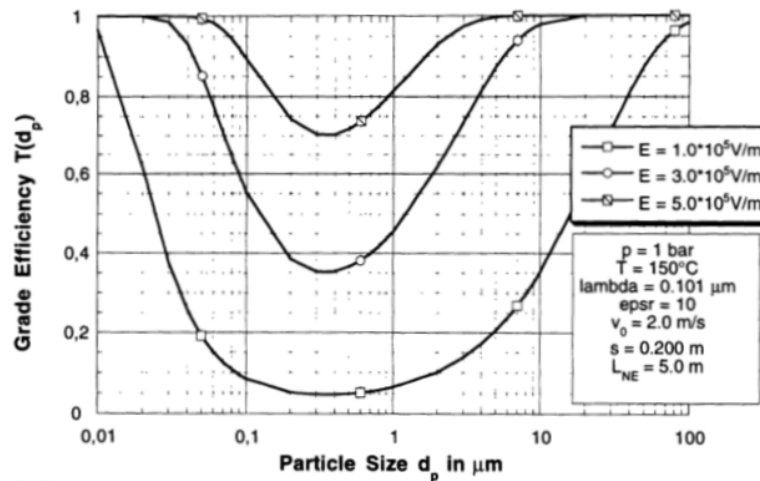
FIGURE 4.10: Demonstration of the strong influence of electric field strength on grade efficiency [5]

Other experiments, have also demonstrated that low velocities outperformed higher ones. That was the case for a similar ESP, where the grade efficiency was higher also on the minimum points around 0.35 μm if the precipitator is operated at 0.5 m/s, than if it is operated at 1.5 m/s.

Effective Migration Velocity. It has been discuss the important role of partial efficiency for different particle sizes. However, an overall efficiency E is still valuable to evaluate the overall efficiency of the ESP.

The drift velocity of the particles is a very important parameter, as particles require a determined residence time, so that the electrical field charges them, and this is regulated by the velocity.
For that, a new magnitude is introduced, which characterizes mass transfer, called *effective migration velocity* (eq. 4.23), and it serves as an overall average efficiency, because it measures the "mass transfer". Effective migration velocity w_{eff}, differs from the previously explained theoretical migration velocity w_{th}, in that it is an overall average of the

velocity of *all* the particles. As oppose to theoretical migration velocity, which is individual to each particle, as it depends on time, on particle size diameter and on the mass of the particle (see eq. 4.14), consequently theoretical migration velocity is different for different particle sizes. The only case where theoretical and effective migration velocity are equal, is when there is monodispersion, i.e. all the particles have exactly the same size.

$$w_{eff} = -\frac{\dot{V}}{A_{NE}} \cdot ln(1 - E_3) \tag{4.23}$$

$$E_3 = 1 - exp\left\{-w_{eff} \cdot \frac{\dot{V}}{A_{NE}}\right\} \tag{4.24}$$
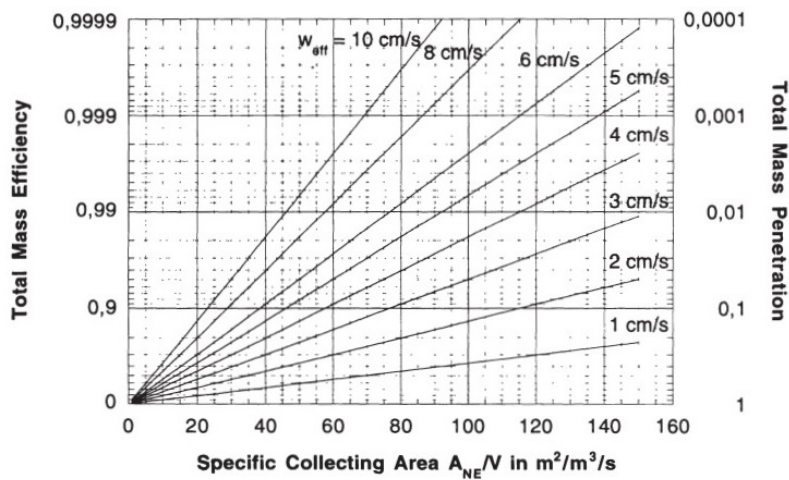
FIGURE 4.11: Dependence of total mass efficiency on specific collecting area for different effective migration velocity w_{eff} values [5]

The total mass efficiency depends on the geometry, particularly on the *specific collection area*,which is the area of the collecting plates over the volume flow rate, and on the overall velocity of the particles. Total mass efficiency here represented on a logarithmic scale (fig. 4.11), as the effective migration velocity is an exponential, it results in an straight line. This straight line can overpredict performance for locations further down the duct, as there the concentration of dust particles have reduced.

Larger particles are easier to collect, and are collected on the first sections of the duct, so the ones remaining further in the flow are smaller and have lower transport velocities which is linked with lower efficiency. This is due to the fact, that for smaller particles as they have less surface area, the probability of collision with the electrons that would deflect its trajectory towards the collecting plate, is smaller than for larger particles. For this reason, effective migration velocity is not constant throughout the whole duct, as

concentration changes (decreases) with location. To account for that a correction factor can be introduced and the *modified effective migration velocity* w_k (eq. 4.25) cam be obtained.

$$w_k = -\frac{\dot{V}}{A_{NE}} \cdot (-ln(1 - E_3))^{1/k} \tag{4.25}$$

$$E_3 = 1 - exp\left\{-(w_k \cdot \frac{\dot{V}}{A_{NE}})^k\right\} \tag{4.26}$$

Effective migration velocities on typical large ESP are around $0.04 - 0.2\ m/s$, one order of magnitude smaller than the theoretical migration velocity. This is why the two concepts should not be confused, and compared, as they measure different things. In fact, an increase in the drift velocity of the particles, correlates with a decrease of the effective migration velocity, and therefore of the overall efficiency.

An increase in duct spacing, specifically duct width (plate-to-plate distance $2s$), with the same velocity, results in a higher effective migration velocity, and therefore an increase in total mass efficiency. This is because having a larger area, allows a higher volume of particles travelling thought the same space, so the mass flux is increased and also the mass transfer.

Mass flux Although effective migration velocity w_{eff} is widely used, it could be confusing or misleading, due to its name with the theoretical drift velocity of the particles w_{th}, that's why mass flux will be explained. The *total collected mass flux* ($j_{m,c}$), i.e. the particles per unit time and area, that are trapped in the collectors, describe the precipitator's efficiency in a clearer way than the effective migration velocity.

To measure the overall efficiency of a precipitator, as the main objective of the ESP is to filtrate the particles, the simplest approach to evaluate this, is to measure the difference between the *total particle mass flow* (i_m) that is desired to be filtered at the entrance $i_{m,e}$, and the remaining unwanted particle mass flow at the exit $i_{m,f}$ (eq. 4.28). The total particle mass flow trapped on the collectors is $i_{m,c}$ and the particle mass flow concentration $c_{m,e}$ (eq. 4.27) allow to estimate the efficiency E_3 in a precise manner. The subindexes m, c, e and f stand for $mass, collected, emitted$ and $final$ respectively.

$$i_{m,e} = c_{m,e} \cdot \dot{V} \tag{4.27}$$

$$i_{m,c} = i_{m,e} - i_{m,f} = i_{m,e} \cdot E_3 \tag{4.28}$$

This approach to measure efficiency can be difficult to perform outside the lab. That is why, although a simpler and more intuitive method to measure efficiency than the effective migration velocity, it can be less practical due to technical issues. Anyways, it accurately characterizes the total precipitation capability of the apparatus. Total collected mass flux $j_{m,c}$ explicitly depends on mass concentration c_m, and it is described by equation 4.29:

$$j_{m,c} = c_{m,e} \cdot E_3 \cdot \frac{\dot{V}}{A_{NE}} = c_{m,e} \cdot E_3 \cdot \frac{v \cdot s}{L_{NE}} \tag{4.29}$$

4.2.4   Dust deposition

When the dust particles, deflected from the straight horizontal trajectory of the flow, by the charge carriers, eventually collide with the grounded collecting electrode, the electrical charge detaches from the particles. As the particles can no longer move because they have found a physical barrier, the electrons of the charge carriers flow through the collecting electrode until ground (see fig. 4.12).
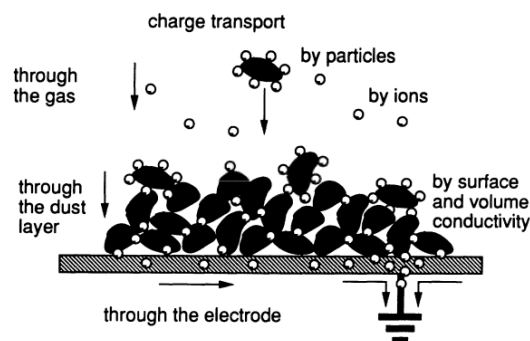
FIGURE 4.12: Dust deposition and charge particles passing through the dust layer to the collecting plate [5]

The charge carriers driving the dust particles, are not the only one that end up on the collecting electrode, also all those charge carriers that did not found a dust particle. These free electrons also have to pass through the dust layer deposited on the surface of the collecting electrode. A higher current will mean a higher flow of charge carriers, which can increase the precipitation efficiency, but depending on the dust resistivity of the particles, it could also lead to a back-corona, which would mean a failure of the system. That is why intermittent high voltage pulsating systems are often use, as it results in a lower total charge carrier flow, without decreasing efficiency, and also they require less energy than a continuous flow [5].

4.2.5 Dust removal

The removal of the dust from the precipitator duct, in one-stage plate-type dry ESPs, can be done while on operation. This poses a problem, which is that the electrical current still flowing through the dust layer holds the dust layer like an electrical glue, this needs to be broken up. For that, a mechanical impact in the way of hammers activated in certain time steps break the dust layer into agglomerations which setle into hoppers.

Another problem associated with simultaneous operation and removal, is that some already collected fine particles can re-enter the flow, as the dust layer breaks. This depends on the turbulence of the flow, and can reduce the efficiency of the ESP.

As the particles being filtrated in the case of this thesis are not harmful for the environment, the hoppers can release the accumulated dust on the ground, either directly from a cavity at nacelle level, or though a conduit, at the feet of the WECS structure.

Chapter 5

Case Study

5.1 Introduction

In this section, the climatic conditions present on the Arabian Desert will be described and a specific place will be selected. Its climatic characteristics will be explained and a comparison adapted to this conditions will be made, between a mesh-fiber filter and an electrostatic precipitator filtration system in a WECS. This comparison will be in terms of performance as well as a cost analysis.

All deserts have similar characteristics among them, such as being dry, arid and mostly inhospitable places. Although most of them are close to the equator, differences in location and proximity to the sea or ocean will lead to differences in the environmental characteristics. As so, the solution proposed in this thesis pretends to address the main issues that the common desert climatic conditions burden in WECS nacelles. But, since there are not exact universal conditions shared in every dessert location, this thesis will focus on the ones from an specific site, (Dhahran) in Saudi Arabia, so that the climatic data used for the description of the problem is accurate and real, not a simple guess. This thesis pretends to give a realistic solution to real problems, and thus, the author hopes that the solution provided to the general problem in a specific site can be later extrapolated to solve the same or similar set of problems on a different site, with similar characteristics, mainly in the Middle East and North Africa (MENA) region.

Saudi Arabia is the largest country in the Middle East, and the Arabian Desert covers more than half of the total area of the country. Even though on a different continent, the Arabian Desert can be considered a specific region or a continuation of the Sahara

Desert. The biggest differentiator between the two, is that the Arabian Desert is sur-
rounded by the Indian Ocean, which could play an important role on the less fluctuation
of temperature, between day and night, giving a more stable temperature in the Arabian
Desert compared with the high variance of ambient temperature over the same day in the
Sahara [-40, 50] ºC. The average maximum temperatures in the Arabian Desert range
from 40º to 50º in Summer, depending on the elevation, and the average minimum tem-
peratures are 20 ºC in Summer and 10 ºC in Winter [21].

5.2 Site selection

After an assessment of the different regions inside the Saudi Arabia desert, one is se-
lected and its specific conditions are used for the study of the problem in this thesis.
Based on the previous work of M.A. Baseer and S. Rehman [7], which used a multi-
criteria decision making (MCDM) approach, based on geographical information systems
(GIS) modeling, developed a map (Figure 5.1) of the most suitable places for developing
a wind farm in Saudi Arabia. This modelling took into account not just climatic conditions,
such as ambient temperature, wind speed and altitude; but also key parameters for the
suitability of building a wind farm in a specific place, such as the electrical network and
road infrastructure; population centers, in order to leave buffer zones between them to
avoid negative effects, such as noise and visual pollution near this centers; slope, rivers,
water bodies, ecological sites, and railways. All this parameters where weighted accord-
ing to the author's criteria and a map was generated, which represents in a color scale
from 1 (less suitable), to 6 (most suitable) the best place to install a wind farm. The map,
as pointed out by the authors, indicates mainly three regions for wind farm development
in Saudi Arabia: (1) Al-Wahj in the west coast, (2) Al-Jouf near the northern border with
Jordan, and (3) the eastern region near the coastal cities of Ras Tanura, Damman and
Dhahran.

The site selected for this thesis will be the last one (3), the eastern region, near the coastal
city of Dhahran, as on other publications, such as [22–24] it has also been described as
one of the most suitable places, since it has the highest average wind speed in the country
[22].
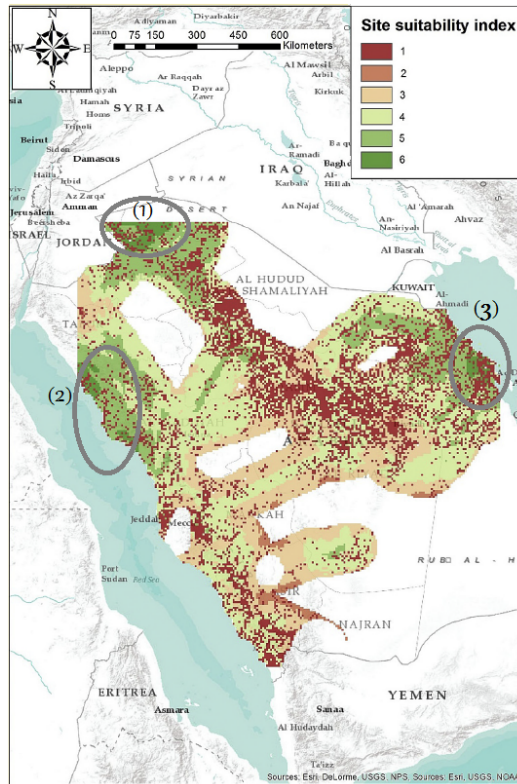
FIGURE 5.1: Wind farm site suitability [7]

5.2.1 Wind speed and wind frequency

According to the Saudi Arabia Wind Atlas [7], the average wind speed in Dhahran, measured at 10 m AGL, is 4.42 m/s and its Wind Frequency Histogram superimposed with the solid curve which is the Weibull fit (fig. 5.2), as calculated by [22], is:
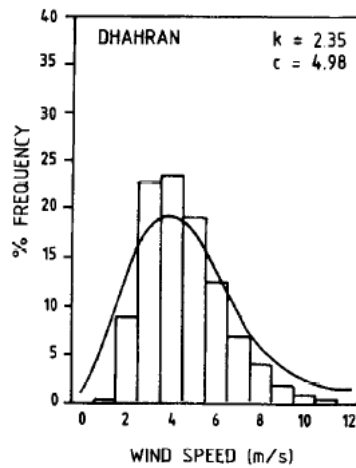
FIGURE 5.2: Dhahran Wind Frequency Histogram at 10m AGL

As wind turbine nacelles are placed at a height that ranges from 60 to 140 m, I find useful the interpolation made by [7] from 10 m to 100m using Hellmann's power law (eq. 5.1) to find out the wind speed at 100 m, using the Dhahran known information at 10 m AGL. Hellmann's power rule states that:

$$V_2 = V_1 \left(\frac{Z_2}{Z_1} \right)^n \tag{5.1}$$

Where V_1 and V_2 are the wind speeds at height Z_1 and Z_2 respectively and n is the value of wind shear coefficient, which is assumed as 1/7 for open land [25]. In fact, Rehman et al. [7], already made a map with this the interpolation at 100 m AGL for the entire country of Saudi Arabia (see Appendix A: figure A.1).

So when applying Hellmann's rule to the Dhahran wind frequency histogram, the obtained distribution is shown in Figure 5.3, and the most common wind velocities at 100 m height can be observed to be between $6 - 7$ m/s.
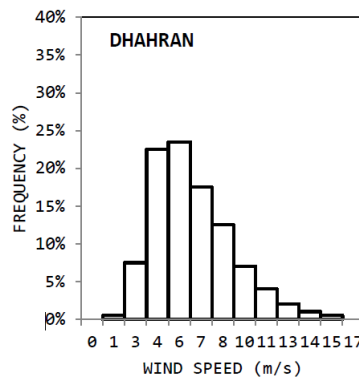
FIGURE 5.3: Dhahran Wind Frequency Histogram at 100m AGL

It might be important to note, as found out by H. Khonkar [23] that the wind speed, on the Arabian Gulf, is stronger in winter than in summer. The winter season lasts from November to March and reaches its maximum during December to February.

5.2.2 Temperature

The mean and average peak temperatures recorded on the Dhahran King Abdulaziz Air Base, situated approximately 40 km from the selected site are displayed on table 5.1. In this case the registered maximum temperature on average does not reach 50ºC, although it does in some occasions, in certain days of the hottest months. So 40 ºC should be the

selected temperature for the design of a cooling system for a WECS nacelle placed in this location. As explained before, the cooling system has to be designed based on the summer temperatures.

Temperature °C			
	Mean		
Month	Max	Min	Mean
1	21.2	10.2	15.4
2	23.2	11.9	17.2
3	27.2	15.0	20.7
4	33.2	19.9	26.1
5	39.6	25.0	32.0
6	42.7	27.7	35.0
7	43.9	29.2	36.1
8	43.2	29.0	35.6
9	40.8	25.8	32.7
10	36.5	22.3	28.9
11	29.5	17.2	22.9
12	23.8	12.6	17.8

TABLE 5.1: Mean and Average Peak Temperatures in Dhahran

5.2.3 Air dust and sandstorms

A special set of characteristics of the desert environment, are their sandy dunes and spectacular sandstorms. But how frequent are they, and how much dust/sand does the air carries with it when the wind blows at high and moderate velocities? To answer this questions, the definitions of these weather phenomena is given:

- The World Meteorological Organization defines blowing dust (or sand) as: "An ensemble of particles of dust or sand raised, at or near the observation site, from the ground to small or moderate heights by a sufficiently strong or turbulent wind." [26]

- The World Meteorological Organization defines dust storms or sandstorms as: "An ensemble of particles of dust or sand energetically lifted to great heights by a strong and turbulent wind."[26]

It can be observed that the difference between these two phenomena is based on the severity and impact of the wind energy.

Regarding the difference between dust storm and sandstorm, professor M. Almazroui,

director of the Center of Excellence for Climate Change Research in KAU, distinguishes a dust storm from a sandstorm in the basis of particle size. Sandstorms are made of large particles that range from 0.08 mm to 1 mm in diameter, while dust storms are made up of a multitude of fine particles, which size ranges from 0.1 μm to 6.0 μm. It also notes a difference in height reached by the particles of these phenomena, as sand particles are confined to the lowest 3.5 m, rarely reaching more than 15 m above ground; dust particles can be elevated up to 3 km [27].

As commercial WECS nacelles placed at hub height can be considered on average, higher than 15 m, a focus on dust storms size particles, rather than on sandstorms particle size, will be given in this thesis, as they reach higher altitudes, and because, as reported by M. Almazroui, "dust particles also stay in the atmosphere much longer time that large particles and can remain airborne for 30 days if it reached a height of 1 km and no other vertical acceleration occurs" [27]. This depends obiously on particle diameter, being true the affirmation for particles under than 0.1 μm; around 14 days for particles between $0.1 - 1.0$ μm and ; and being of around 1 day for particles between $3.0 - 6.0$ μm.

According to the meteorological station placed in Dhahran King Abdulaziz Air Base, the number of days that these two special weather phenomena, Dust Blowing and Sand-storms, occur over a year are 68 and 3.5 days respectively (Table 5.2).

Month	Blowing Dust	Dust/Sand Storm
1	4.0	0.3
2	6.0	0.2
3	6.9	0.7
4	7.1	0.6
5	9.4	0.8
6	10.5	0.4
7	10.0	0.2
8	4.4	0.1
9	2.3	0.0
10	1.7	0.1
11	2.9	0.1
12	2.8	0.0
Total	68.0	3.5

TABLE 5.2: Number of days with occurrence of different weather phenomena in Dhahran

5.2.4 Precipitation and humidity

Precipitation is the magnitude that measures rainfall. It is measured in SI units mm, which refers to the amount of rain per square meter in one hour, captured in the rain gauge (instrument for the measurement of rainfall). One millimeter of rainfall is the equivalent of one liter of water per square meter. Precipitation is not very common in Dhahran, as only in 53 days of the entire year some level of precipitation occurs. A map of the annual rainfall in Saudi Arabia is included in the Appendix A, fig. A.2.

Relative humidity, refers to the ratio of the partial pressure of water vapor to the equilibrium vapor pressure of water at a given temperature. Relative humidity changes with temperature, and as the temperature rises on the hotter months, relative humidity decreases to the mid thirties; the opposite happens on the cooler months, where average mean relative humidity can reach the high sixties (Table 5.3).

The levels of relative humidity in Dhahran are high, characteristic of a coastal site, maybe uncommon on other desert parts, but as seen on the suitability map (figure 5.1) and the average wind speed map (figure A.1), two of the three most suitable places for wind farms and with higher average wind speeds are located on the coast of the country.

Month	Precipitation (mm)	Relative Humidity (%)
1	17.4	68
2	12.6	64
3	16.8	57
4	5.0	48
5	1.0	36
6	0.0	32
7	0.0	35
8	0.0	46
9	0.0	51
10	0.1	59
11	15.3	62
12	17.7	68

TABLE 5.3: Average precipitation and mean relative humidity in Dhahran

5.2.5 Particle Size

In a paper by [8], a measurement of the dust size distribution according to height is performed, at 1, 6, 15 and 21 m in the capital of Saudi Arabia, Riyadh. Although Riyadh

is not the selected place, this kind of data is scare and hard to access, so this data will be extrapolated for this thesis study up to 100 metres height, by a power rule (eq. 5.2 given by the author of this paper, and the data will be assumed to be equal on the place selected (Dhahran).

The relation between the average particle size diameter D_{av}, and the height H in meters is given, and it can be concluded that, the average particle diameter of the distribution decreases as height increasing, according to equation 5.2:

$$D_{av} = D_0 \cdot H^{-\alpha} \tag{5.2}$$

It is difficult to establish a global distribution during storms and the distribution may depend on the location and the storm conditions. It can be concluded that, each sand/dust-storm may have different particle size distribution, and that this distribution is also height dependent as well.

The average diameter decreases consistently with the increase of height; as can be seen in figure 5.4. The variation of diameter at higher altitudes is lower than at lower heights. For example, D_{av} varies from 42.5 μm to 21 μm at a height of 1 m compared with a variation from 16 μm to 18.4 μm at a height of 21 m. It is likely that larger particles have higher fall velocity and settle down rapidly while smaller size particles can rise to higher levels and remain suspended for a relatively appreciable time.
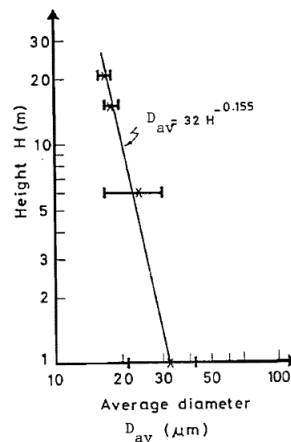
FIGURE 5.4: Variation of the average diameter Dav with height H [8]

For the higher height tested in the experiment, 21 m, the particle size distributions fit in most cases a normal distribution, being the average size diameter at this height of 16.8μm.

Using the mentioned equation (5.2), the average particle size diameter at 100m has been estimate to be 15.67 μm. Thus, the most probable size class at 100 metres is the one between 10-20 μm, so it will be the size class to which this thesis filtration system should adapt.

5.3 Selected WECS

The WECS selected for this project is the Vestas V112. This WECS has been selected because an abundance of information related with the technical aspects being studied here has been found, mostly its refrigeration system. It has a power of 3 MW, the blade diameter is 112 m and the hub height is 94 m.

This WECS is different to most others in the market, for the placement of the heat exchanger at the top rear of the nacelle (see fig. 5.5). This heat exchanger is referred as *CoolerTop*. It is part of the primary cooling system, it exchanges the heat of the internal cooling liquids (oils and water) conducted to the CoolerTop via electrical pumps. For the secondary cooling system air enters the nacelle through the air intake on the bottom of the nacelle. The dimensions of the nacelle are:

Width	4.12 m
Length	12.8 m
Height	3.4 m
Height* (incl. CoolerTop)	6.9 m

FIGURE 5.5: Vestas V112 3MW [9]

The CoolerTop of the Vestas V112 is a free flow cooler, which means that there are no electrical components from the refrigeration system outside of the nacelle exposed to corrosion. There are two Liquid Cooling Systems that refrigerate the different internal components of the nacelle. The first one serves the gearbox and the hydraulic system, and the second one serves the generator and the converter. The heat extracted from the components via the refrigerant liquid is taken using an electrical pump to the CoolerTop. The transformer, in this WECS is placed in a different room behind the generator. It is cooled with forced air cooling, using a fan located at the bottom of the nacelle, that through a duct directs the air between the high voltage and low voltage windings of the transformer. Depending on the WECS design sometimes the transformer is placed inside or outside the nacelle, so its refrigeration will be neglected in this study.

The nacelle internal temperature, needs to be maintained at operational levels, therefore the heat emitted by the internal components (generator, gearbox and converter), which isn't captured by the cooling liquids of the primary cooling system, results in hot air inside the nacelle, which is evacuated from the nacelle through two fans located at the sides of the nacelle. The airflow of outside air enters the nacelle through an air intake in the bottom of the nacelle [28].
This airflow, which is exposed to ambient particles, is what the filtration system in this thesis will study, as it is the most prone to damaging the internal components of any WECS placed in the desert.

5.3.1   Heat Load

The heat load of this 3 MW WECS, is derived from the heat loss that the internal components need to dissipate to properly function. These components are the gearbox, the generator and the electrical equipment.
Following a recent study for WECS in the Sahara desert at extreme temperatures (45 °C) for a similar a WECS of 2.5 MW, the heat load can be assumed to be 3 %, 12 % and 1 % respectively for the gearbox, the generator and the electrical equipment [29]. The simulations were performed at 12 m/s which resulted in electricity generation at rated power. Adapting these values for the selected 3 MW wind turbine in this thesis, the total heat load is of 480 kW (see table 5.4).

From this heat load, 80-90% is evacuated by the primary cooling system, (according to Vestas internal information) the heat load which the secondary cooling system has to evacuate for the ventilation of the nacelle is between 10 and 20 % of that heat load.

	%	kW
Gearbox	3	90
Generator	12	360
Electrical Equipment	1	30
Total	**16**	**480**

TABLE 5.4: Heat load for a 3 MW at extreme conditions (T=45ºC and v=12m/s)

Therefore, 80 kW (17% of the total heat load) will be assumed for the comparison calculations.

5.3.2 Ventilation System

The interior of the nacelle requires a ventilation system, so that the air inside is renovated, with forced air cooling, substituting this air heated by convection from the internal components, with cleaner air from the outside. This ventilation system is part of the secondary cooling system. It shouldn't be confused with the the main secondary cooling system heat exchanger, the CoolerTop, which uses natural air cooling.

The nacelle has a volume of $5380\ m^3$, according to [30], the air needs to be renovated depending on the function of the space, in this case the nacelle's function has been assumed to be that of a machine room, which need 20-30 renovations of air each hour. The maximum volume flow rate, results from multiplying the volume of the air inside by the maximum renovations per hour needed, and it is a volume flow rate of $Q = 5400\ m^3/h$. This figure, agrees with the manufacturer value of $5700\ m^3/h$ [31], and will be the one that the fan must be able to cover.

The ventilation system of the nacelle is composed of a central fan placed in the floor of the nacelle, through which the airflow enters, and two smaller fans situated on the sides of the nacelle, through which the air exits.The inlet fan has a diameter of $1.05\ m$ and the two lateral fans have a diameter of $0.55\ m$. The specific fan used in this WECS nacelle model, has not been found, but the dimensions from a fan also used by Vestas for other models have been assumed [32].

The filtration system will be designed for this bottom inlet fan, with an area A_{fan} of $0.866\ m^2$. As the flow rate is the velocity times the cross sectional area, the intake velocity of the fan v_{fan} has to be $1.73\ m/s$ (see eq. 5.3).

$$v_{fan} = \frac{Q}{A_{fan}} = \frac{1.5\ m^3/s}{0.866\ m^2} = 1.73\ m/s \tag{5.3}$$

5.4 Design of the ESP

To the author knowledge, there are no existing WECS which use an Electrostatic Precipitator for their filtration system. It has been observed by the author that the majority of air intakes in commercial WECS are either on the top or the bottom of the nacelle. In this case the air intake is on the floor of the nacelle, therefore the proposed ESP will be placed there, to be as close to the air inlet as possible.

The design of the ESP has been done, starting from the base of typical characteristic values of ESP operation according to [5]. But overall it is an experimental design based on the theoretical principles of electrostatic operation explained in chapter 4. As the space is limited, the first magnitude to be designed has been the geometry of the simplest ESP duct, that in case of being insufficient, additional ducts could be mounted next to it. Then, the radius of the discharge wire has been selected, and proper electrical parameters have been calculated adjusted to these physical values. Ultimately the power consumption has been calculated to later compare it with that of a conventional mesh-fiber filter.

5.4.1 Dimensions

The designed plate-type ESP is a rectangular duct with a plate-to-plate spacing $2s$ of $300\ mm$, and equal height. The discharge electrode assumed to be a cylindrical rod, have a wire radius r_{SE} of $1\ mm$. The wire-to-wire spacing $2c$ is the same as the wire-to-plate spacing s of $150\ mm$, to obtain maximum efficiency. With this dimensions and following the equation 4.5b, the characteristic value d is equal to $521.04\ mm$.

The designed ESP has a square profile, and a width of $0.3\ m$. The cross sectional area of the ESP duct is therefore, $0.09\ m^2$. Doing a mass balance (eq. 5.4), and neglecting a change in the air density, the flow rate at the intake of the ESP and at the intake of the fan has to be the same. If only one duct, with a cross sectional area of $0.09\ m^2$ was used, having the same flow rate than the fan, but an area 9 times smaller, the velocity inside the ESP would be $16.67\ m/s$, completely unsuitable for ESP operation. Therefore, if a similar velocity for the ESP to that of the fan is wanted, so that it is suitable for ESP operation, but the area of the duct is approximately 9 times smaller, 9 ESP ducts are needed. These ESP ducts, will be referred units, and will be mounted in a 3 by 3 matrix, in order to optimize the space (see fig. 5.6).
Actually 9.62 ducts would be needed for the velocity of the airflow inside the ESP units
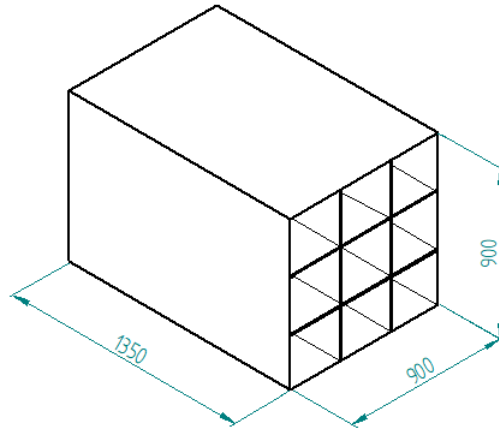
FIGURE 5.6: ESP with 9 units

to be equal to that of the fan. Due to geometry constrains, only 9 instead of 10 ducts are selected, and therefore, the airflow velocity inside the ESP ducts v_0 will be $1.85\ m/s$, well within the typical values for plate-type ESPs of $1 - 2\ m/s$.

$$\dot{m}_{in} = \dot{m}_{out} \tag{5.4}$$

$$\dot{m} = \rho \cdot Q = \rho \cdot v \cdot A \tag{5.5}$$

The length of the ESP has been selected according to a common industry aspect ratio. The ratio is the effective length to the effective height of the collector surface. As there are three ESP mounted one on top of each other, the effective collector plate height is the sum of the three ducts height, $0.9\ m$ in total. The aspect ratio AR in ESPs with high efficiencies should be greater than 1.0, usually between 1.0 and 1.5 [33].

$$AR = \frac{Length}{Height} \tag{5.6}$$

An aspect ratio of 1.5 has been selected, so the length of the ESP L_{NE} is $1.35\ m$. Therefore, each plate will be of $0.9x1.35\ m$, thus, each having an area of $1.215\ m^2$. Overall, the total collecting area A_{CE} of the ESP is $7.29\ m^2$ (eq. 5.7). There are 4 plates, the two outer ones, and the two inner ones. The inner plates are shared by the center column of the ESP units, and the outer columns next to it, so the collecting area of the inner plates is doubled.

$$A_{CE} = 1.35\ x\ 0.9\ x\ 6 = 7.29m^2 \tag{5.7}$$

Summarizing, all the explained ESP dimensions and the flow rate are listed in table 5.5.

Parameter	Sym.	Value	Magnitude
Plate-to-plate distance (unit width)	2s	300	mm
Wire-to-plate distance	s	150	mm
Wire-to-wire distance	2c	150	mm
Wire radius	r_{se}	1	mm
Cross sectional Area	A_c	0.09	m^2
Number of discharge wires per unit	N_{SE}	9	-
Number of ESP units	N_{units}	9	-
Number of collecting plates	N_{CE}	4	-
Effective Width	W_{eff}	900	mm
Effecive Height	H_{eff}	900	mm
Length	L_{NE}	1350	mm
Aspect Ratio	AR	1.5	-
Collecting Area	A_{CE}	7.29	m^2
Airflow velocity	v_0	1.85	m/s
Total Flow Rate	Q	5400	m^3/h

TABLE 5.5: Geometrical parameters of the designed ESP

5.4.2 Electrical Parameters

With this geometry and a wire radius r_{SE} of $1\ mm$, corresponds a corona onset voltage V_0 of $35\ kV$. Modifying equation 4.4, the corona initiation field strength can be calculated (see eq. 5.8), which results in E_0 equal $5.56\ KV/cm$. A little over the typical E_0 values of $3.5 - 4\ kV/cm$.

$$E_0 = \frac{V_0}{r_{SE} \cdot ln(\frac{d}{r_{SE}})} \tag{5.8}$$

The electrical state of the ESP and thus, the power consumption of the corona will, depend on the gas flow rate that it has to ionized. Under these conditions, which are within the typical characteristic values of ESP operation, to achieve around 99.0% efficiency the power consumption of an ESP depending on the flow rate, according to [5], is around $170\ W$ of DC power for each m^3/s . In this case, with a volume flow rate Q of $5400\ m^3/h$, the power consumption of this ESP P_{ESP} is around $255\ W$.

This value seems realistic, compared to a similar experiment [31], in where a much shorter $0.75m$ tube-type ESP, designed for the same function had a design power consumption of $131.5W$. As mentioned above, the ESP has been divided into 9 ducts, and so has the flow rate, each one with a gas flow rate Q_i of $600\ m^3/h$. This power consumption figure of the corona is a simplification, as a detailled corona power consumption would be much more complex and outside the scope of this thesis.

5.4.3 Adaption of the ESP

The ESP will be mounted on the bottom outside the nacelle. For the air filtrated by the ESP, to enter the nacelle ventilation through the fan situated at the floor of the nacelle, an outlet nozzle, similar to an elbow is necessary, so that the fan absorbs the airflow from the ESP. This would require a structure, that houses the ESP and seals the nacelle from outside unfiltered air. Such an adaption, could be something similar to a box as depicted in fig. 5.7. The material is assumed to be the same of the nacelle, glasfibre. Maybe a more aerodynamic design could be achieved, but this is outside the scope of this thesis, as well. This structure will be assumed for the sake of simplicity.

The structure consists of a glasfibre squared box, with the same area of the fan, that would be $1050x1050mm$, and would protrude from the nacelle bottom face, the same height as the plate type ESP, that would be $0.9\ m$. This box would have an opening in one side to allow the ESP outlet airflow to enter, and would have another opening om its top face that, is in contact with the nacelle, as that is where the fan is located.
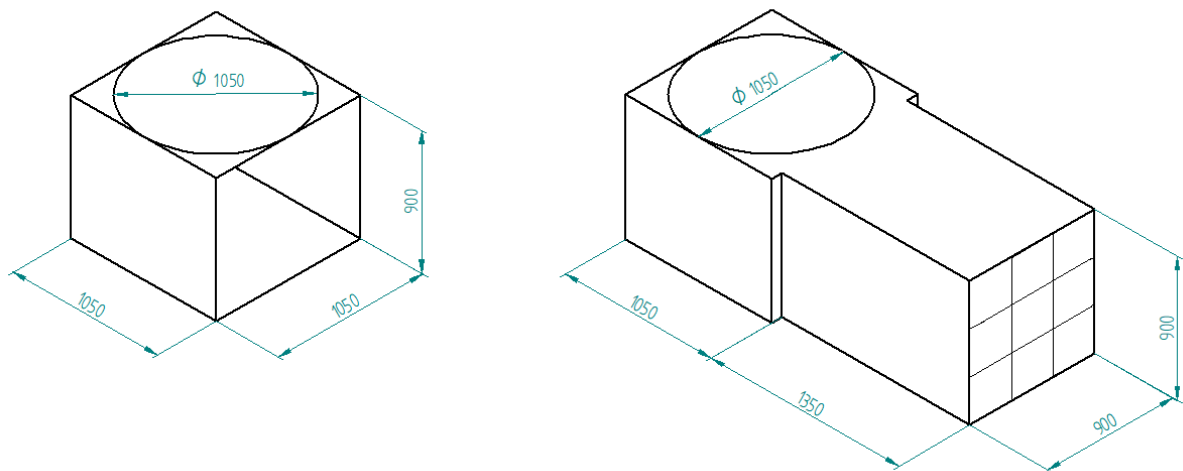

FIGURE 5.7: ESP and the adpater box

5.5 Performance comparison between mesh-fiber filters and ESPs

5.5.1 Assumptions

In this section, a performance comparison will be made for the designed ESP and a mesh-fiber filter for the ventilation of a WECS for particles between $10-20$ μm. There will be two cases, the most extreme one, at maximum flow rate, for which the ESP has being designed, and a more common one, at the minimum flow rate.

- **CASE 1**: When wind speeds are over 12 m/s and the WECS is generating electricity at rated power 3 MW (see fig. A.3), corresponding with the maximum air renovation per hour needs: 30 renovations per hour ($Q = 5400\ m^3/h$).

- **CASE 2**: At a lower, more common power generation of 1 MW, corresponding with a wind speed of 7 m/s and the minimum air replacement needs of the nacelle: 20 renovations per hour ($Q = 3600\ m^3/h$).

The energy consumption of the fan E_{fan} depends on many variables (see eq. 3.10), like volume flow rate, pressure difference, time of operation and the efficiency of the fan. As mentioned before (section 3.5), the efficiency of the fan is assumed to be 70 %, and the fan time of operation t is assumed to be the same of the operation time of the WECS, 2700 hours.

The pressure drop has been assumed to be 220 Pa for the filter, as particles over 10 μm are assumed for this study. According to the standard EN779, these particles are considered coarse dust.
For the Electrostatic Precipitator, the pressure drop has been assumed to be 40 Pa for Case 1, and 20 Pa for Case 2. These values have been obtained according, to the flow rate, from a table provided by a manufacturer of an ESP with similar dimensions [34].
One consideration that has not been taken into account has been the pressure drop of the elbow, that redirects the airflow from the ESP outtake to the fan inlet.

5.5.2 Results

With all the values set (table 5.6), the total energy consumption E_{Total} over an operating time of $2700\ h$ will be equal to the energy consumed by the fan E_{fan} for the filters, and for

Parameter	Symbol	CASE 1	CASE 2	Magnitude
Flow rate	Q	5400	3600	m3/h
Power consumption	P_{ESP}	255	170	W
	P_{filter}	0	0	
Pressure drop	Δp_{ESP}	40	20	Pa
	Δp_{filter}	220	220	
Operation time	t	2700	2700	h
Efficiency	η_{fan}	0.7	0.7	-

TABLE 5.6: Data

the ESPs, the consumption of the fans E_{fan} has to be added to the energy consumption of the ESP E_{ESP} (see eq. 3.11).

As it can be observed from table 5.7 and figure 5.8, even for the most demanding case, Case 1, over one year of operation there is an energy saving of 27,73% when using an ESP. And in the more common one, Case 2, the savings are 36,87%. These results validate the use of an ESP to substitute a mesh-fiber filter for the filtration of air going into the nacelle, from a performance point of view. In addition to that, the filtration efficiency for ESPs is higher and it doesn't change over time, as it does for mesh-fiber filters, as dust builds up on it over time.

FIGURE 5.8: Energy Consumption
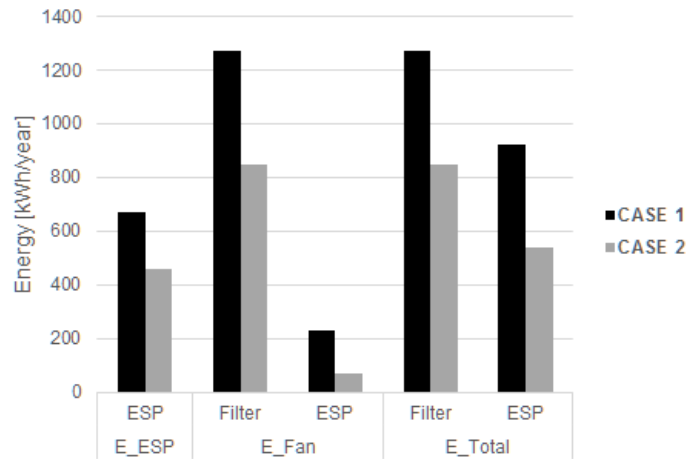
	E_{ESP}	E_{Fan}		E_{Total}	
	ESP	Filter	ESP	Filter	ESP
CASE 1	689	1273	231	1273	920
CASE 2	459	849	77	849	536

TABLE 5.7: Energy Consumption [kWh]

5.6 Cost-benefit analysis

It has been shown in the previous section how, electrostatic precipitators can save up energy for a WECS, which,means that the overall performance of the WECS increases, as less energy has to be spent on the secondary ventilation system. The savings of around 300 kWh every year for both cases, do not seem like much for a 3 MW WECS, as they roughly make about 1 % of the total energy produced by the WECS in a year. So more aspects, other than performance will be examined in this section, with the realization of a cost analysis.

As explained in section 3.5.2 the total cost C_{Total} of a filtration system is composed by the sum of its parts. These parts are:

- C_{CI} The Capital Investment cost

- $C_{O\&M}$ The Operation & Maintenance cost

5.6.1 Capital Investment Cost

The Capital Investment cost C_{CI} for the experimental ESP design presented here, accounts for the structure and material used, as well as some additional equipment needed for the ESP to work. The installation cost of the ESP has been neglected, as it would ideally have been attached to the WECS nacelle before it is placed in position at hub height, otherwise it could be economically prohibitive.

To estimate the cost of the ESP, some general guidelines from the American *Environmental Protection Agency* (EPA) [35] have been followed. One important acknowledgement, is that although the EPA does not recommend to extrapolate its data for precipitators of smaller sizes such as this one, but due to the lack of information available, this was the most accurate and detailed source found. Real values from more advanced designs in the market vary much depending on size and application. All in all, the EPA guidelines have been followed regardless, as it was the best source available.

Another consideration to be taken into account is that the data provided by the EPA is giving in 1987 $, so they will be adjusted for inflation to 2018 $, and then converted to €
to make a proper estimation of costs.

The proposed ESP is a plate-type ESP, which is formed by the collecting plates, which typically are made of carbon steel, but for better reliability and durability, stainless steel has been selected. This increases the base cost of the ESP by 30%.

There are 9 ESP units, which share 4 plates, the two outer plates, and the two inner plates. As explained before (section 5.4.1, eq. 5.7), the total collecting area A_{CE} is equal to $7.29\ m^2$ (in imperial units $78.46\ ft^2$).

If a 20 \$/ft^2 ratio is assumed [35], the total base cost is \$1570 (in 1987 \$). This means that the minimum "flange-to-flange" cost is around €3100 today (2018)[1]. To this, some basic equipment has to be added, such as thermal or electrical insulation, which can add up 10% of the base cost; or inlet and outlet nozzles, such as the adapter structure mentioned in section 5.4.3, this can add up another 10 %. In addition to the stainless steel construction mentioned before, and some electrical equipment for the control of the precipitator operation, which can represent up to 8 % of the cost. Hoppers have not been added to the design, since the collected dust is not made of polluting substances and therefore can be directly evacuated back to the environment.

Item	Cost Adder, %	Cost [€]
Base Cost	-	3100.00
Stainless steel construction	30	930.00
Insulation	10	310.00
Inlet and oulet noozles	10	310.00
Equipment	8	248.00
Total Capital Investment Cost		**4898.00**

TABLE 5.8: ESP Capital Investment Cost

All these cost adders are presented in table 5.8 and the total Capital Investment Cost estimation adds up to €4898 (in 2018 €), which will be rounded to €5000, a conservative estimation, for a precipitator of this size.

For the mesh-fiber filters, the capital investment cost, can be assumed to be the same as the cost of buying a new replacement of the filters, around €120. Considering them to be installed on the nacelle also when it is manufactured, so the installation cost can also be neglected. It won't be neglected however when it will have to be replaced, which will be explain in the next section, as part of the O&M cost.

---

[1] To do this conversion, the 1987 \$ have been adjusted for inflation to represent 2018 \$. \$1 in 1987 represents the purchasing power of \$2.21 in 2018 [36]. Then, these 2018 \$ have been converted into 2018 € at the current rate of \$1 = €0.89.

5.6.2   Operation and Maintenance Cost

The Operation & Maintenance Cost $C_{O\&M}$ is calculated in a per yearly basis, in order to see if the operation and maintenance cost of the ESP system are in fact lower than those of the mesh-fiber filter system. And if they are lower, compute the savings each year, and the years needed to make up for the ESP larger Capital Investment cost.

The **operation cost** accounts for the cost of the total energy that the ventilation system consumes E_{Total}. This cost is given in a per year unit, the energy consumed in a year times the price of the energy. As mentioned in section 3.5, the price of energy selected is €0.040/kWh.

From the two cases explained in the performance analysis, the case selected for the cost analysis is Case 1, where the ventilation system with ESP consumed 920 kWh, and the one with mesh-fiber filters consumed 1273 kWh. Therefore, the annual operation cost adds up to €36.80 for the ESP system and €50.92 for the one with filters (see table 5.9).

	Filter	**ESP**
Energy [kWh]	1273	920
Cost of operation [€]	**50.92**	**36.80**

TABLE 5.9: Cost of Operation

For the **maintenance cost**, the lifetime of the filter L_{Filter} is a key variable. As it can vary a lot, and its influence on the analysis is very determining, a sensitivity analysis is proposed to assume the filter's lifetime. In this analysis 3 situations are presented, depending on the dust concentration in the air, which will determine how often the filters have to be replaced:

- Situation 1, low dust concentration, where the lifetime of the filter is assumed to be 1 year. Thus, the annual frequency of replacement will be 1.

- Situation 2, medium dust concentration, where the lifetime of the filter is assumed to be 6 months. Thus, the annual frequency of replacement will be 2.

- Situation 3, high dust concentration, where the lifetime of the filter is assumed to be 4 months. Thus, the annual frequency of replacement will be 3.

The area that needs filtration is equal to the the air intake area, a 1 m^2 intake. As the majority of the filters found, have dimensions around 500 mm, 4 filters are needed in

each replacement. The price for these filters have been found to be around €30. So if the price of each filter is assumed to be €30, each replacement adds up to €120. The annual replacement cost will depend on how often these filters need to be replaced.

The ESP has no disposable parts, and thus it is assumed to not need replacements. The only maintenance needed is a yearly revision by a technician, which can be neglected, as the manufacturer of the nacelle, already does yearly inspection of its WECS.

Concept	Cost [€]
Individual Labor cost	75.00
4 Technicians	350.00
Displacement Cost	200.00
Total Labor Cost	**500.00**

TABLE 5.10: Labor Cost for each replacement

The price of labor can vary hugely on the location of the wind farm, the number of technicians needed and the experience of these technicians. To estimate the **cost of labor** C_{Labor} for the replacement of the filters, the hourly salary of the technician is multiplied by the hours that it will spend working in a particular task. In this case, it has been assumed that the operator has a monthly wage of €3000, working 20 days each month, with a typical 8 hours workday, which makes an hourly wage €18.75.

If each replacement is assumed to take on average 4 hours, that means that the individual labor cost of one technician is €75 for each replacement. If several technician, lets say a group of 4, need to travel to the wind farm site, the costs of displacement or transportation also has to be included. The total labor costs for each replacement has been estimated to be €500 for each replacement (see table 5.10).

This estimated value seems reasonable for the relatively simple task of replacing a filter, and maybe it can even be an underestimation compared to the €750 per WECS maintenance, reported in [37], which also takes into account other aspects such as pensions, offices or training, whcih have been neglected in this thesis for the sake of simplicity.

5.6.3 Total Cost

Taking into account all the factors discussed, the total annual cost for the first year is presented in table 5.11. The three situations mentioned in the previous section, can have a great impact in the annual costs of filtration system, tripling the O&M cost $C_{O\&M}$, in the most dusty situation.

The different parts that make up the total cost are listed in the table 5.11, first showing

the parts that make up the maintenance cost, replacement and labor cost. Then, the two parts that make up operation and maintenance cost. Finally the O&M cost and the Capital Investment cost are added to give the Total Cost.

Cost	Filter			ESP
	Situation			-
	1	2	3	-
Replacement Cost	120.00	240.00	360.00	-
Labor Cost	500.00	1000.00	1500.00	-
Maintenance Cost	620.00	1240.00	1860.00	-
Operation Cost	50.92	50.92	50.92	36.80
O&M Cost	670.92	1290.92	1910.92	36.80
Capital Investment Cost	120.00	120.00	120.00	5000.00
Total Cost	**790.92**	**1410.92**	**2030.92**	**5036.80**

TABLE 5.11: Cost Analysis

After year 1, the Capital Investment cost of purchasing the ESP doesn't have to be taken into account. That, means that the capital investment cost, does not repeat every year for both the Filter and the ESP. To find out whether the ESP is a better option, than the mesh-fiber filter, from an economical point of view, the total cost over the years have to be compared correctly.

To properly do so, for example in year 3, the total cost would amount to € 5114.40 for the ESP, and to € 2132.68 for the filer in the less dusty situation, situation 1. This calculation is done multiplying the O&M cost by the number of years that have passed, and adding the capital investment cost of year 1 (eq. 5.9) to find out how much has been spent up to that date.

$$C_{Total,year\ i} = C_{CI,year\ 1} + \sum_{i=1}^{n} C_{O\&M,year\ i} \tag{5.9}$$

As it can be observed in table 5.12, after 5 years the total cost of having an ESP amounts to € 5184.00, which is cheaper than the total cost of owning a filtration system with mesh-fiber filters in situations 2 and 3. However, in situation 1 where there is less dust, and the filter have to be replaced less often, the mesh fiber filter would be more economical than the electrostatic filtration system.

5.6.4 Results

As the ESP has been assumed to not have any maintenance cost, with all the assumptions taken, the ESP has been found to be more economical overall for all 3 situations, regardless of dust concentration.

Time	Filter			ESP
	Situation			
	1	2	3	
Year 1	790.92	1,410.92	2,030.92	5,036.80
Year 3	2,132.76	3,992.76	5,852.76	5,110.40
Year 4	2,803.68	5,283.68	7,763.68	5,147.20
Year 5	3,474.60	6,754.60	9,674.60	5,184.60
Year 8	5,487.36	10,447.36	15,407.36	5,294.36
Year 10	6,829.20	13,029.20	19,229.00	5,368.00

TABLE 5.12: Total Cost over the years

- For situation 3, in very dusty places the ESP becomes cheaper than the filters after just 3 of operation.

- For situation 2, in what has been considered moderately dusty locations, the ESP becomes slightly cheaper than the filters after 4 years of operation.

- For situation 1, in lower dusty locations, the ESP doesn't become cheaper than the filters until the 8th year of operation.

Over a span of 10 years, the total economical savings of owning an ESP, compared to the mesh-fiber filters, can be estimated to be 21% for situation 1, 60% for situation 2, and 72% for situation 3.

5.7 Case Study Conclusions

For the selected location for the placement of a WECS, near the city of Dhahran, in Saudi Arabia it can be concluded, that the substituion of mesh fiber filters, for the air filtration on a WECS nacelle, with an Electrostatic Precipitator can be plausible.

Depending on the conditions, like the dust concentration, the wind availability and the cost and lifetime of the filters or the ESP; from the study carried out in this chapter, ESPs can be considered a viable alternative to mesh fiber filters.

Chapter 6

Socio-economic Impact

6.1 Social Impact

Developing countries outside the West, may have difficulties adapting technology originally designed on the West. Specially if the climatically conditions are substantially different, as it is the case in countries situated in the MENA (Middle East and North Africa) region (figure 6.1). The environment of this countries, is dominated, mostly by the desert. This harsh environment and other reasons, historical, political and economical, may explain the poverty of the region, in general.
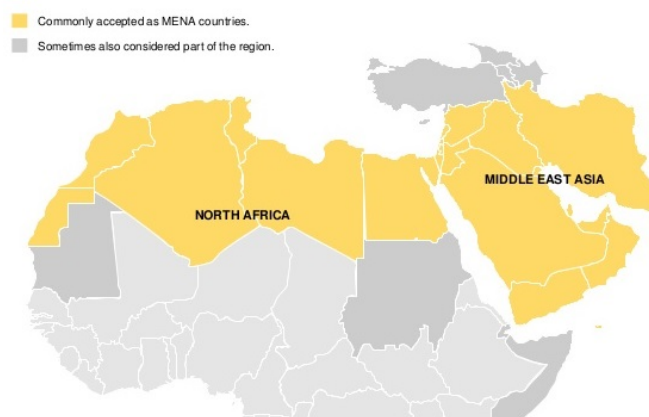

FIGURE 6.1: Middle East and North Africa

Some of these countries however, have became rich in the last decades thanks to findings of oil and natural gas reserves on their underground (Qatar, UAE, Kuwait or Saudi Arabia). This allowed them to jump start their economies and the development of their citizens,

using the benefits of selling oil and natural gas. However, it is know that fossil fuels are limited and determined to run out. This will impact their energy mix and their economic model. This is one of the reasons, as it is also environmental consensus over the benefits of using not polluting cheaper and renewable energy, why their governments have taken action and designed and funded programs to develop their future energy mix, making it less dependent on fossil fuels.

Saudi Arabia, the country selected for this study has designed a plan: *Saudi Arabia Vision 2030*, a government initiative to reduce its dependence on oil and diversify its economy. The target set by the plan is to reach 54 GW of renewable energy power installed capacity by 2030, of which 9 GW will be wind energy. The development of the plan, according to the Saudi government, would reduce emissions from power plants of CO_2, NO_X and SO_2 by 60%, 75% and 70% respectively; also, alternative energy employment opportunities would contribute USD 51 billion to the country's GDP, and create 137,000 direct employment opportunities [38].

The improvement of the WECS technology in the set of rich countries, can be later used on the poorer countries on the region, with similar conditions, once technology has been enhanced and cheapened. This would help, the need of all the countries in the region, as their energy demand increases, as the region's population grows and develops.

6.2 Economical Impact

The economical impact of the study has a great potential, in a broader scale, helping to improve the ventilation and filtration system of WECS in the region. In a more concrete sense, it can save millions of dollars to the owner and operator of a wind farm in Saudi Arabia.

The economical impact will be calculated in terms of the money saved, by not having the WECS out of operation, due to the maintenance associated with the replacement of the mesh-fiber filters. In this sense, it is assumed that each WECS can be up to 1 week out of operation, from the moment that the filter is considered to be full, i.e. the dust cake is so thick that the pressure drop over the filter is too big for operation, until the moment the filter is replaced. This 1 week delay is reasonable, due to the fact, that the technicians or company responsible with the replacement of the filters, have to travel to the wind farm, and send the new filters, and also the fact, that if in a normal wind farm there are 15-20

WECS, the filters of all the WECS cannot be replaced on the same day. Therefore, 1 week out of operation due to maintenance time associated only with the replacement of the filter seems a reasonable assumption.

Taking as a reference, the average cost of electricity in Saudi Arabia, that is the average price of electrical energy generation in the country, the potential losses for the owner of the wind farm associated to not having the WECS working for one week due to the maintenance of the filters will be calculated. The average cost of electricity in Saudi Arabia (in USD) is 2.48 cents/kWh [39]. If the WECS is out of service for one day the potential daily losses are $5,356 (eq. 6.1).

$$Daily\ Losses = 30\% \cdot 3MW \cdot \frac{1 \cdot 10^6 J}{1\ s} \cdot \frac{3600\ s}{1\ h} \cdot \frac{24\ h}{1\ day} \cdot \frac{1\ kWh}{3.6 \cdot 10^6 J} \cdot \frac{\$0.248}{kWh} = \$5,356/day$$
(6.1)

For the calculation of the WECS output is done with the same capacity factor of 30%. This means that on average the WECS would only be producing electricity at 3 MW one third of the hours of a day. This is a more realistic assumption than simply assuming that the WECS is generating electricity at rated power 24 hours a day for a whole week.

A single day economical loss, equals the estimated capital investment cost of the proposed ESP, around $5,000. A whole week would amount to $37,500 only for 1 WECS. If in a typical wind farm there are between 15-20 WECS, the potential savings of having a filtration system that does not require at least 1 week of maintenance every year, could be estimated to be between $500,000 and $750,000 every year.

The beneficial impact that the replacement of the mesh-fiber filters could have on the profitability of wind energy in dusty desert climates is therefore considered theoretically proven, and to have a very positive impact on the region.

Chapter 7

Conclusion

In this thesis, a study of the of the different WECS cooling technologies has been made and it has been found out that, although for big WECS over 1 MW, the liquid cooling system is the most appropriate primary cooling system, some commercial WECS, like the one studied here, still utilized forced air cooling, which needs to be filtered, to ensure the longevity of the internal parts of the nacelle.

A study of the different particle collection mechanism that could be employed for the filtration system of WECS nacelles in a desert climate, has been done, and it has been concluded that the two most viable options for this purpose are mesh-fiber filters and ESPs. In addition to that, a methodology to be able to compare both system has been given.

The study of ESPs have shown the basic principles of operation of electrostatic precipitation, which has led to the desgin of small scale experimental precipitator. This design, has been adapted for the filtration needs of a WECS ventilation system, and it has been compared in terms of performance and in terms of costs.

The finding of this analysis have been that the usage for ESP in a filtration system can end up saving energy overall, around 30% of the energy consumed by the ventilation system each year. Although ESPs consume electricity to operate, the reduction in fan electricity consumption is considerable enough, due to the lower pressure drop of ESPs, to result in a more energy efficient system than one with mesh fiber filters.

Regarding the cost analysis, under the assumptions taken and the conditions of the study, the ESP has been found to be cheaper in the long term, compared with the mesh fiber

filters. Three different situations have been presented, depending on the dust concentration in a given location and therefore on the lifetime of the filters. Even for the less dusty place, the ESP has been found to have a lower total cost than mesh fiber filters, during a span of 10 years. Although mesh-fiber filters do have a much lower capital investment cost, than ESPS, their higher operation and maintenance cost has resulted in a higher overall cost in the middle and long term.

The viability of substituting mesh-fiber filter for ESP and the impact that the future development and implantation of this technology could have on desert environments is considered proven. The operator's estimated economical savings, of one theoretical wind farm have been found to be at least $1 million, for only one year.

Finally, the author of this thesis believes that the project has been successful. However, more research is needed in this field, to develop cheaper ESPs, as well as better estimations regarding its power consumption and maintenance cost. Overall, this is just the author's grain of sand, so that others can advance the impact of renewable energies in less favored climates, and reduce the world's dependence of fossil fuels.

Appendix A
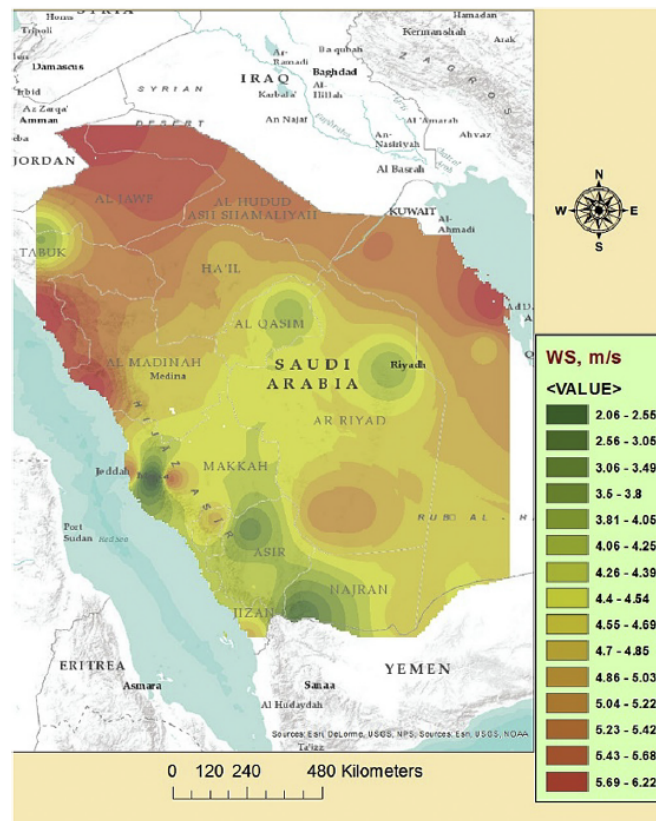
Appendix A: Additional Information

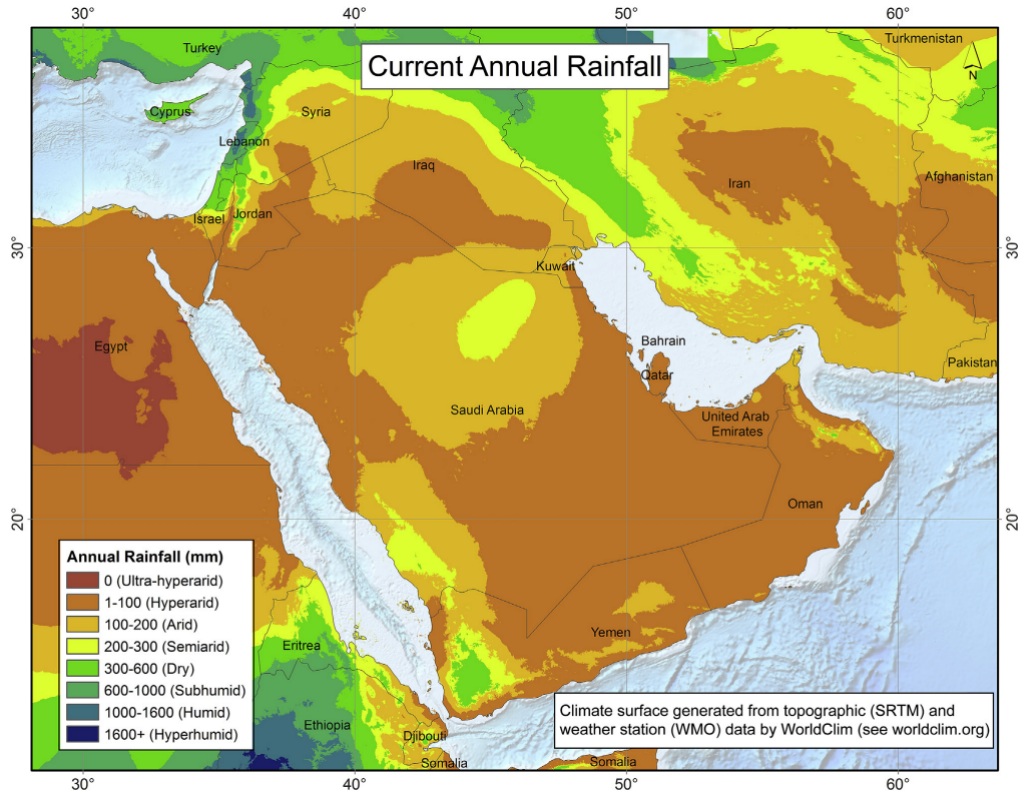FIGURE A.1: Saudi Arabian map interpolated with wind speed at 100m AGL [7]

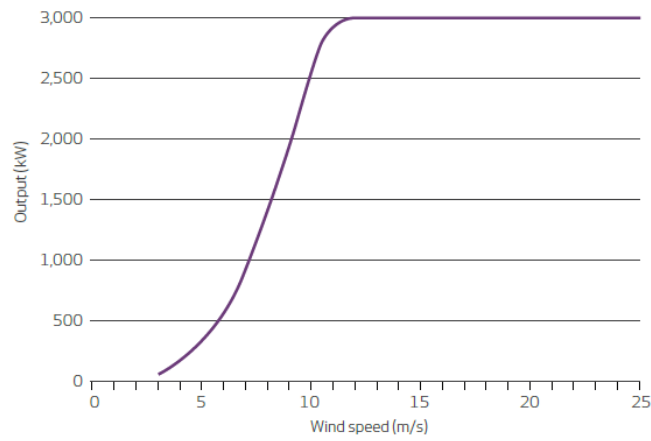FIGURE A.2: Current Annual Rainfall in Saudi Arabia

FIGURE A.3: Vestas V112 3.0 MW Power Curve [10]

Bibliography

[1] Wind Europe. Annual combined onshore and offshore wind energy statistics. *Wind in Power 2017*, February 2018.

[2] Global Wind Energy Council. Globañ wind report 2018. April 2019.

[3] Y. Jiang. *Wind Power Generation and Wind Turbine Design*, chapter 19: Wind turbine cooling technologies. WIT Press, 2010.

[4] N. M. Bojdo. Rotorcraft engine air particle separation. Master's thesis, University of Manchester, 2012.

[5] C. Riehle. *Applied Electrostatic Precipitation*, chapter 3: Basic and theoretical operation of ESPs. Chapman Hall, 1997. ISBN 0-7514-0266-4.

[6] Nazaroff and Alvarez-Cohen. Electrostatic precipitator. URL `https://www.dartmouth.edu/~cushman/courses/engs37/ESPs.pdf`. [Online] Accessed: 03-06-2019.

[7] J.P. Meyer M.A. Baseer, S. Rehman and Md. Mahbub Alam. Gis-based site suitability analysis for wind farm development in saudi arabia. *Energy*, October 2017.

[8] A. A. Ali A. S. Ahmed and M. A. Alhaider. Analysis of particle size distribution during sand/dustorm in riyadh, saudi arabia. *Atmospheric Environment*, 21, 1987.

[9] Wind-Turbine-Models.com. Vestas v112 onshore. URL `https://en.wind-turbine-models.com/turbines/7-vestas-v112-onshore`. [Online] Accessed: 01-05-2019.

[10] Vestas. V112 3.0 mw, one turbine for one world. URL `https://www.niko-brno.cz/files/V112-30.pdf`. [Online] Accessed: 09-06-2019.

[11] C. Masson A. Smaili, A. Tahi. Thermal analysis of wind turbine nacelle operating in algerian saharan desert. *Energy Procedia 18*, October 2012.

[12] C. Shuying S. Jian, M. Xiaoqian and G. Huijing. Review of the cooling technology for high-power wind turbines. *5th International Conference on Advanced Design and Manufacturing Engineering (ICADME)*, 2015.

[13] A. V. Mamishev T. Wen, I. Krichtafovitch. The key energy performance of novel electrostatic precipitators. *Journal of Building Engineering*, 2:77–84, 2015.

[14] C. Wadnpohl W. Peukert. Industrial separation of fine particles with difficult dust properties. *Powder Technology*, 118:136–148, 2001.

[15] T. Caesar. Air filter classification in the light of rising energy costs. *Feudenber Filtration Tecnologies KG*, 2008.

[16] J. A. Navarro Martinez. Diseño preliminar de un aerogenerador de 3 mw. Master's thesis, Universidad Politécnica de Madrid, 2010.

[17] K. R. Parker. *Applied Electrostatic Precipitation*. Chapman Hall, 1997. ISBN 0-7514-0266-4.

[18] Z. Al-Hamouz. Numerical and experimental evaluation of fly ash collection efficiency in electrostatic precipitators. *Energy Conversion and Management*, 79:487–497, 2014.

[19] R. Feynman. The feynman lectures of physics, vol. i. URL `http://www.feynmanlectures.caltech.edu/I_41.html`. [Online] Accessed: 09-12-2018.

[20] A. Sleigh C. Noakes. "real fluids" an introudction to fluid mechanics. URL `https://web.archive.org/web/20101021003853/http://www.efm.leeds.ac.uk/CIVE/CIVE1400/Section4/laminar_turbulent.htm`. [Online] Accessed: 04-01-2019.

[21] timeanddate.com. Annual weather averages in dhahran. URL `https://www.timeanddate.com/weather/saudi-arabia/dhahran/climate`. [Online] Accessed: 13-08-2018.

[22] T. Husain S. Rehman, T. O. Halawani. Weibull parameters for wind speed distribution in saudi arabia. *Solar Energy, Vol. 53, No 6*, pages 473–479, 1994.

[23] H. Khonkar. Complete survey of wind behavior over the arabian gulf. *Journal of King Abdulaziz University (JKAU) - Science, Vol. 20*, pages 31–47, March 2009.

[24] M. A. A. Mohamed H. M. Farh, A. M. Eltamaly. Wind energy assessment for five locations in saudi arabia. *International Conference on Future Environment and Energy (IPCBEE), Vol. 28*, pages 48–55, 2012.

[25] Gilbert M. Masters. *Renewable and Efficient Electric Power Systems*. John Wiley Sons, Inc, 2004. ISBN 0-471-28060-7 (cloth).

[26] Word Meteorological Organization (WMO). International cloud atlas. URL `https://cloudatlas.wmo.int/dust-storm-or-sandstorm.html`. [Online] Accessed: 2018-08-31.

[27] M. Almazroui. Climatology and monitoring of dust and sand storms in the arabian peninsula. *Center of Excellence for Climate Change Research (CECCR), King Abdulaziz University (KAU)*, 2017.

[28] Vestas Wind System. General specification v112-3.0 mw. URL `https://stopthesethings.files.wordpress.com/2015/12/vestas-v112-specs.pdf`. [Online] Accessed: 05-05-2019.

[29] K. Nuri Tekin T. Yavuz and E. Koç. Thermal analysis of wind turbine nacele of 2,5 mw turbine at severe weather conditions. *6th International Congress of Energy and Environmental Engineering and Management, Paris*, July 2015.

[30] E. Carnicer Royo. *Ventilación Industrial. Cálculo y Aplicaciones*. Editorial Paraninfo S.A., 1991. ISBN 84-283-1891-3.

[31] A. Donado Arroyo. Simulación cfd de un precipitador electroestatico de particulas (esp) en una turbina eólica. Master's thesis, Universidad Carlos III de Madrid, 2018.

[32] HYDAC Cooling System Ecotecnia. Sparesinmotion.com, vestas fan search results. URL `https://www.sparesinmotion.com/search/fan/brand/vestas`. [Online] Accessed: 13-05-2019.

[33] Neundorfer.com. Esp design parameters and their effects on collection efficiencys. URL `https://www.neundorfer.com/wp-content/uploads/2016/05/ESP-KnowledgeBase-03-Design_Parameters.pdf`. [Online] Accessed: 16-05-2019.

[34] Tecna. Crystall - filtro electrostatico 900. URL `http://www.tecna.es/images/pdfadjunto/CRYSTALL.pdf`. [Online] Accessed: 24-05-2019.

[35] U.S. Environmental Protection Agency. Epa lessons. URL `https://ppcair.com/products-services/electrostatic-precipitation/dry-esp`. [Online] Accessed: 19-05-2019.

[36] Official Data Foundation. Inflation calculator. URL `http://www.in2013dollars.com/1987-dollars-in-2018?amount=1`. [Online] Accessed: 30-05-2019.

[37] L. Bertling J. Nilson. Maintenance management of wind power systems using condition monitoring systems—life cycle cost analysis for two case studies. *IEEE TRANSACTIONS ON ENERGY CONVERSION, VOL. 22, NO. 1,*, March 2007.

[38] IRENA (International Renewable Energy Agency). Building the renewable energy sector in saudi arabia. URL `https://www.irena.org/-/media/Files/IRENA/Agency/Events/2012/Sep/5/5_Ibrahim_Babelli.pdf`. [Online] Accessed: 05-09-2018.

[39] M. Anwer and W. Matar. Reforming industrial fuel and residential electricity prices in saudi arabia. URL `https://www.kapsarc.org/research/publications/reforming-industrial-fuel-and-residential-electricity-prices-in-saudi-arabia`. [Online] Accessed: 10-06-2019.